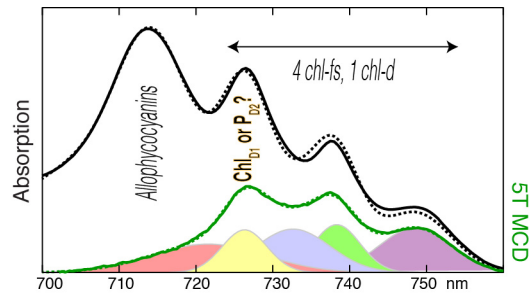**TOC Graphic**

Highlights

- Primary Donor confirmed at 726 nm
- Determination of far-red chl pigment Q_y excitation positions, widths, CD and MCD amplitudes
- Quantification of electrochromic shifts and $Q_A^{\bullet-}$ photoconversion yield
- Electrochromic shift consistent with primary donor at either Chl_{D1} or P_{D2}
- The CD amplitude favors the primary donor at P_{D2}

`

The primary donor of far-red Photosystem II: Chl_{D1} or P_{D2}?

Martyna Judd[1], Jennifer Morton[1], Dennis Nürnberg[2], Andrea Fantuzzi[2], A. William Rutherford[2],

Robin Purchase[1], Nicholas Cox[1] and Elmars Krausz*[1]

[1] Research School of Chemistry, Australian National University, Canberra 2600, Australia

[2] Department of Life Sciences, Imperial College, London SW7 2AZ, United Kingdom

Corresponding Author
*Elmars Krausz email: elmars.krausz@anu.edu.au

Running Head: FR-PSII Primary donor

Keywords: photochemistry, photochemical charge separation, exciton coupling, Circular Dichroism, Magnetic Circular Dichroism, fluorescence, electrochromic shift.

Abbreviations:
Canonical chlorophyll-a based Photosystem II - chl-a-PS II
Far-red light grown PS II - FRL-PS II
Circular Dichroism - CD
Magnetic Circular Dichroism - MCD
chlorophyll-a - *chl-a*
chlorophyll-d - *chl-d*
chlorophyll-f - *chl-f*
Far-red light chlorophyll (chlorophyll-d and/or chlorophyll-f) - FRL-chl
Supplementary Information – SI

ABSTRACT

Far-red light (FRL) Photosystem II (PSII) isolated from *Chroococcidiopsis thermalis* is studied using parallel analyses of low-temperature absorption, circular dichroism (CD) and magnetic circular dichroism (MCD) spectroscopies in conjunction with fluorescence measurements. This extends earlier studies (Nurnberg *et al* 2018 Science 360 (2018) 1210-1213). We confirm that the chlorophyll absorbing at 726 nm is the primary electron donor. At 1.8 K efficient photochemistry occurs when exciting at 726 nm and shorter wavelengths; but not at wavelengths longer than 726 nm. The 726 nm absorption peak exhibits a 21 ± 4 cm^{-1} electrochromic shift due to formation of the semiquinone anion, $Q_A^{\bullet-}$. Modelling indicates that no other FRL pigment is located among the 6 central reaction center chlorins: P_{D1}, P_{D2} Chl_{D1}, Chl_{D2}, $Pheo_{D1}$ and $Pheo_{D2}$. Two of these chlorins, Chl_{D1} and $P_{D2,}$ are located at a distance and orientation relative to $Q_A^{\bullet-}$ so as to account for the observed electrochromic shift. Previously, Chl_{D1} was taken as the most likely candidate for the primary donor based on spectroscopy, sequence analysis and mechanistic arguments. Here, a more detailed comparison of the spectroscopic data with exciton modelling of the electrochromic pattern indicates that P_{D2} is at least as likely as Chl_{D1} to be responsible for the 726 nm absorption. The correspondence in sign and magnitude of the CD observed at 726 nm with that predicted from modelling favors P_{D2} as the primary donor. The pros and cons of P_{D2} vs Chl_{D1} as the location of the FRL-primary donor are discussed.

1 INTRODUCTION

Oxygenic photosynthesis in the cyanobacteria *Chroococcidiopis thermalis*, when grown in far-red light (FRL), is based on photochemistry occurring on *chl-f* or *chl-d* [1]. This constitutes an unexpected new paradigm in photosynthesis. Photosystem II core complexes (FRL-PS II) of *C. thermalis* contain 4 *chl-f* molecules and 1 *chl-d*, whilst the majority (~30) of the chlorin pigments remain as *chl-a*.

The original spectroscopic studies of the isolated FRL-PS II provided a model in which one of the long wavelength pigments (FRL-chl) played the role of the primary donor, while the 4 remaining FRL-chls served as long wavelength antennas [1]. The primary donor was identified [1] as Chl_{D1} based on the following evidence and arguments: a) trapping of $Pheo_{D1}^{\bullet-}$ at room temperature resulted in electrochromic changes at 720 nm and the apparent loss of the usual dominant blue-shift at ~ 685 nm attributed to *chl-a* Chl_{D1}; b) $Q_A^{\bullet-}$ formation at low temperature resulted in electrochromic changes at 725 nm and again the apparent loss of the usual dominant blue-shift at ~ 685 nm attributed to the *chl-a* Chl_{D1}; c) The presence of amino acid sequence changes in the FRL-D1 protein conserved in all known FRL-D1 sequences, which were modelled as potential H-bond donors to the ring I formyl group of either *chl-d* or *chl-f* in the Chl_{D1} location [1]; d) in *Acaryochloris marina*, a similar bandshift was seen (as well as similar H-bonding amino acids) already attributed to *chl-d* at the Chl_{D1} location [2]; e) functional arguments based on Chl_{D1} taking the primary donor role in canonical *chl-a*-PSII (see e.g. [3-7]); f) The chemical properties of *chl-f* [8] and the redox properties [9] of both *chl-d* and *chl-f* favor its location on Chl_{D1} (see below and [1]).

The reaction center of c*hl-a*-PS II contains 2 *pheo-a* and 6 *chl-a* molecules. P_{D1} and P_{D2} have partial ring overlap, forming a chlorophyll pair that is the counterpart of the "special pair" in purple bacterial reaction centers. The P_{D1}/P_{D2} exciton coupling term in PS II [10] at 158 cm^{-1} is far smaller than the 'special pair' coupling of ~900 cm^{-1} determined for *Rhoropseudomonas viridus [11]*. Chl_{D1} and Chl_{D2} are counterparts of the monomeric bacteriochlorophylls, B_L and B_M, of the bacterial reaction center; they are sometimes anomalously referred to as "accessory pigments" despite the demonstrated role Chl_{D1} (and B_L) has in primary charge separation [3]. The two *pheo-a* pigments, $Pheo_{D1}$ and $Pheo_{D2}$, are also core pigments, with $Pheo_{D1}$ having a key electron acceptor role. $ChlZ_{D1}$ and $ChlZ_{D2}$ are not part of the central group of 6

chlorins as they are peripheral and mainly play light-harvesting roles, although $ChlZ_{D2}$ is part of a side-path electron donation system that works at low quantum yield under some circumstances [12, 13]

P_{D2} was not considered as a candidate for the primary donor role in FRL-PS II although it is oriented and located in a way that can give rise to an electrochromic shift very similar to that calculated for Chl_{D1}. Here we examine the possibility that P_{D2} is the primary electron donor in FRL-PS II.

2 Materials and Methods

FRL-PS II samples were prepared as described in [1].

All spectra were taken on a single, purpose-built multifunctional apparatus [14] built around a 0.75 M Czerny-Turner spectrometer (Spex) and a superconducting magnet cryostat (Oxford Instruments SM-4). The system is able to simultaneously record absorption, CD and MCD spectra at temperatures between 1.8 K and 300 K. This system also can be rapidly reconfigured to measure emission and excitation spectra, without disturbing the cryogenic sample.

The apparatus has a sample handling system [15, 16] that minimizes exposure of the sample to oxygen and ambient light, whilst allowing rapid cooling of a room temperature sample to cryogenic temperatures under controlled conditions. Samples were visualized with a near-IR light (>780 nm) sensitive camera at either room temperature or at cryogenic temperatures. The presence of bubbles, cracks or defects in the prepared sample could be immediately determined without inducing any photoconversion of a dark-adapted sample.

The PSII samples contained cryoprotectant glycerol/ethylene glycol (1:1) at a final concentration of 45 % (v/v). Prior to dark adaption, samples were loaded under low light into specially designed [16] strain-free quartz optical cells of 500 μm, 200 μm or 50 μm pathlength. The PSII samples were then dark-adapted for 5 min before being rapidly cooled.

The light source for the absorption measurements was a highly stabilized 250 W quartz-halogen lamp. The fluence of the measurement light at the sample was reduced to a point that absorption measurements did not induce a significant degree of Q_A reduction in the PS II sample. This was established by determining

that there was no significant difference between two successive absorption measurements. The necessary reduction in measurement light seen by each PS II assembly involved defocusing the measurement light over a large area (~8 mm diameter) sample and narrowing the slit widths of the monochromator, whilst using a large area high quantum efficiency Hamamatsu R 669 photomultiplier to detect the transmitted light [17]. Electrochromism was induced with a highly stabilized 250 W quartz-halogen lamp passed through either a green bandpass filter combined with a 10 cm pathlength water filter to provide 1-2 mW of broad spectrum green light, or through an optical system [14] based on a Spex Minimate 0.25 M double monochromator, providing 6-8 μW of light in the 600 nm - 760 nm range and having a bandwidth of 2.4 nm FWHM (see Fig. S2), or a Schwartz EO Ti:S laser pumped with a 532 nm Continuum Verdi G.

CD and MCD measurements required much higher measurement light levels. It is not possible to measure useful CD or MCD spectra and maintain the sample in the Q_A state [18]. Thus, samples were illuminated with green light (300 s at 1-2 mW/cm^2) forming the $Q_A^{\cdot -}$ state *prior* to the measurement [19] to minimize actinic effects during the course of CD and MCD measurements.

Emission was excited with the highly stabilized lamp and Spex Minimate system described above and then detected through the same 0.75 M Czerny-Turner spectrometer as the absorption with a Hamamatsu R 943-02 photomultiplier tube.

Data were analyzed using IGOR pro software and calculations were made using MATLAB.

3 Results and Discussion

3.1 Canonical chl-a-PS II and FRL-PS II comparisons

Fig. 1 provides a comparison of low temperature spectra of FRL-PS II core complexes of *C*. *thermalis* with those of *T*. *vulcanus*. The latter is a well-determined *chl-a* containing PSII, i.e. *chl-a*-PS II. FRL-PS II exhibits a number of well-resolved absorption features in the 700-760 nm range that are not present in *chl-a*-PS II, as previously reported [1]. Fluorescence spectra of the two systems are also significantly different (Fig. 1 and SI, Fig. S3 of [1]), with *chl-a*-PS II fluorescence peaking near 690 nm and the FR-PS II peaking near 752 nm.
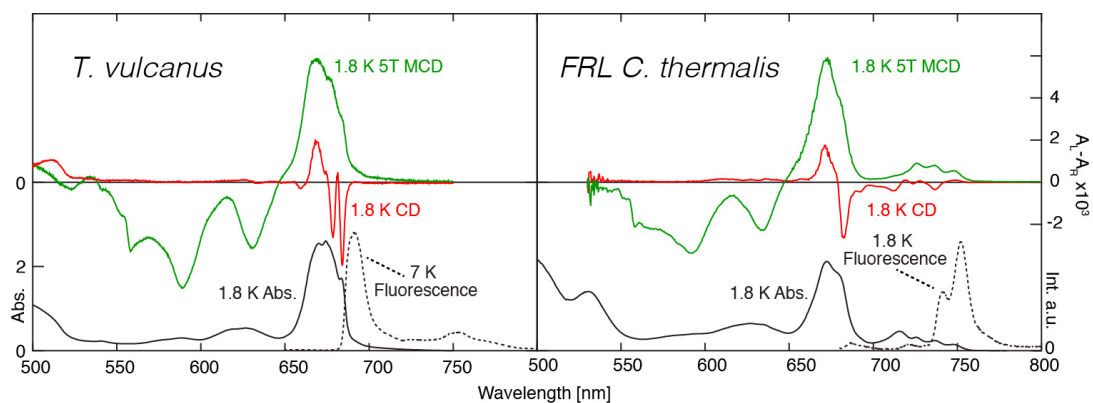
Fig. 1 Low temperature absorption, CD, MCD and fluorescence spectra (as indicated) of chl-a-PS II from T. vulcanus (left, adapted from reference [20]) and FRL-PS II of C. thermalis (right). Corresponding spectra are set to the same integrated Q_y absorption strengths.

Absorption features in the region beyond ~720 nm involve Q_y excitations of 4 *chl-f* molecules and one *chl-d*. Absorption integrals (see SI-1, Fig. S1) are reasonably consistent with there being ~30 *chl-a* molecules, 2 *pheo-a* pigments and 5 far-red chls in FRL-PSII, assuming the oscillator strength of each pigment is similar. This result is in agreement with the direct determination of the pigment content of FRL-PS II from the HPLC analyses as previously reported [1].

3.2 *Identification of the primary donor*

Fig. 2 shows that 735 nm illumination at 1.8 K induces a *minimal* electrochromic shift amplitude near 726 nm. At 77 K, illumination at 750 nm leads to a minimal shift amplitude whereas illumination at 735 nm leads to a small but significant shift amplitude. The small shift at higher temperatures is attributable to the optically excited lower energy pigment (peaking at 738 nm) leading to charge separation by way of thermally activated access to the primary donor at 726 nm. The energy gap between peaks at 726 nm and 738 nm is 12 nm (220 cm^{-1}). This corresponds to ~4 kT at 77 K pointing to a possible thermally activated primary donor occupation of ~2 %. We are thus able to confirm that the 726 nm peak is that of the primary donor [1].
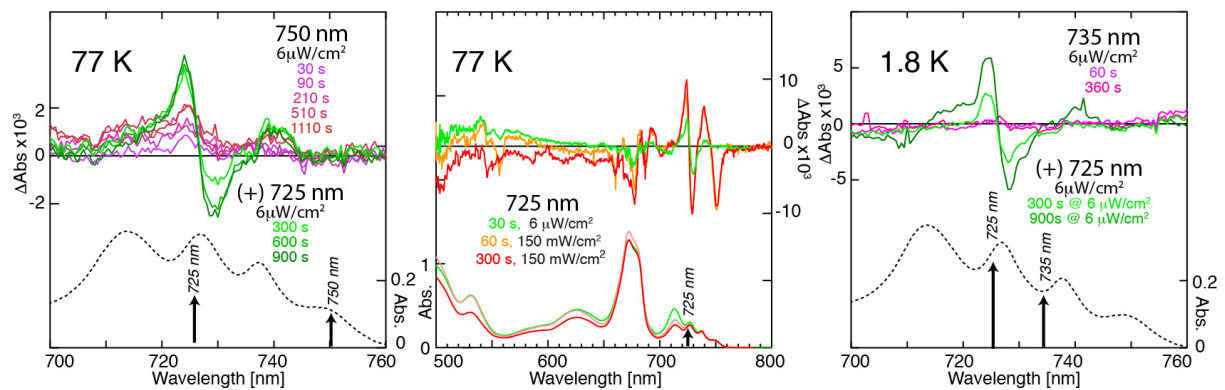
Fig. 2 The left panel shows shift and absorption spectra measured at 77 K, for low power illuminations at 750 nm followed by additional low power illuminations at 725 nm. The central panel compares the 77 K spectrum for a sample illuminated for 30 s with low power 6 μW/cm² 725 nm illumination (green), followed by illumination by a 1500 times more powerful, 150 mW/cm² Ti:S laser, also at 725 nm for 60 s and 300 s (orange and red traces respectively). The right panel shows difference features induced by illuminating at 1.8 K with low power 735 nm radiation, followed by low power 725 nm illumination.

At high excitation fluences, achieved by using a Ti:S laser at 725 nm, additional features are generated in difference spectra (central panel in Fig. 2). Most apparent is a bleach at 749 nm, along with an absorption increase in the 738 nm region. The bleach at 749 nm is associated with partial oxidation of the lowest energy FRL-chl. Such photo-oxidation processes are known [17, 21]. The peak position of the increased intensity component is at 739.5 nm and does not match the peak position of the band seen in absorption. A blue-shift of this type is characteristic of non-resonant photophysical hole-burning [22-24] although such processes are more pronounced at lower temperatures.

3.3 *Variation in allophycocyanin content of FRL-PS II and Global Analysis*

Absorption at wavelengths longer than 700 nm is attributed primarily to FRL-chl. However, there is significant absorption at the shorter wavelength end of the 700 nm to 740 nm region that can be attributed to allophycocyanins [1]. More highly purified FRL-PS II preparations show that the absorption feature near 715 nm becomes depleted, whereas the three other distinct features are retained. Fig. 3 shows FRL-PS II spectra of samples with different allophycocyanin content.
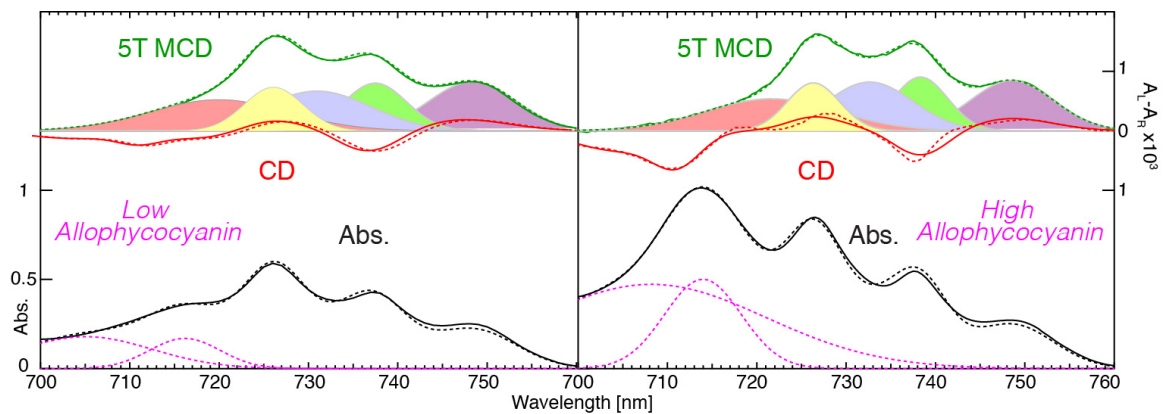
Fig. 3 Absorption (solid black traces), MCD (solid green traces) and CD (solid red traces) of high and low allophycocyanin containing FRL-PS II preparations, scaled to the same area in MCD. A systematic analysis of the MCD (see text and SI-3) leads to the quantification of the 5 individual FRL-chl Q_y MCD components shown in Table S1. The MCD contribution of these 5 Q_y excitons are shown under the MCD spectrum in the figure as coloured overlapping Gaussians. The primary donor (at 726 nm) is yellow. The subsequent fit of absorption spectra (dashed black traces) and CD spectra (dashed red traces), using the positions and widths of the 5 components as determined from the MCD analysis (see text and Table S1) closely follows the experimental data. Allophycocyanin absorption components are estimated (see SI-1) as the dashed magenta curves.

The 700 nm to 715 nm region of FRL-PS II shows little MCD, but significant CD and absorption. The absorption and CD intensity in this region vary strongly with allophycocyanin content (Fig. 3), showing it to be dominated by allophycocyanins. The fluorescence spectra of high- allophycocyanin FRL-PS II (Fig. 1 and SI-2, Fig. S2) exhibit a weak peak near 730 nm, associated with emission from allophycocyanins, indicating that they are, at least partially, disconnected from PSII.

There are three well-resolved peaks in FRL-PSII spectra at wavelengths longer than 720 nm that are not due to allophycocyanins. These are due to the FRL-chls. An analysis of high and low allophycocyanin FRL-PSII samples (Fig. 3, Table S1 and SI-3) establish small changes in the position and width of these peaks, indicating only a minor disturbance of the FRL-PS II proteins associated with the purification process.

The spectral position and width of all 5 FRL-chl Q_y excitations were determined by a parallel, information-driven, global analysis of simultaneously measured absorption, CD and MCD spectra, such as those seen in Fig. 3. The MCD spectra are key to this analysis as they have no significant contribution from overlapping signals from allophycocyanins. Another important characteristic of the FRL-chl Q_y excitations is the MCD

amplitude relative to absorption ratio B/D which in turn is proportional to $\Delta A/A$ at a specific applied magnetic field. This ratio is known to vary and also to be indicative of the role that the pigment takes [18, 25, 26]. The primary donor, in particular, exhibits a narrow Q_y exciton for which its MCD B/D value is significantly reduced (by ~50%) compared to pigments involved in light harvesting, which are less strongly coupled to other chlorophylls [18, 27]. All purely electronic excitations (which include exciton coupled Q_y bands) that exhibit B term-type MCD have line-shapes that follow the absorption profile of each exciton component [28-30]. Each FRL-chl is taken to have the same integrated Q_y absorption intensity. Exciton coupling-induced intensity re-distribution (Section 3.3) is thus considered to be minor. The differences in molar extinction values between *chl-a*, *chl-d* and *chl-f* have been shown [31] to be relatively small in a range of solvents. Computations at the CAM-B3LYP and SAC-CI levels (Table 2 of [32]) provide similar (to within 10%) oscillator strengths for the three chlorins. As an approximation, we take the oscillator strength of *chl-a*, *chl-d* and *chl-f* Q_y excitations in the protein environment to be the same. Whilst individual pigment absorption strengths are similar, the CD amplitude of each Q_y exciton component band can vary in both magnitude and sign, and is determined by exciton coupling to neighboring pigments [33]. For the purpose of this analysis, the CD bandshapes were assumed to be the same as that of the absorption and MCD. However, CD line shapes may follow those of their absorption features less closely when vibrational sideline features become involved [26, 34]. The overall fit to the CD shown in Fig. 3 is less precise than that of the absorption and MCD. This may arise partly as a result of the influence of vibrational sideline CD. Attempts to fit the CD spectrum in the 726 nm region with the CD component of the primary donor constrained to a small relative amplitude were unsuccessful. The positive CD seen in this region is associated with the primary donor (see SI-3 and Fig. S4).

A description of the global analysis is provided in SI-3. Table S1 provides the relevant output. Very similar positions and widths for each FRL-chl Q_y MCD band were obtained from both the low and high allophycocyanin samples shown in Fig. 3. The differences in linewidths between the FRL-chl Q_y features is attributed to a combination disparate levels of inhomogeneity at each pigment site as well as changes in electron-phonon coupling. There is a variation of relatively strong CD features associated with allophycocyanins present in the high and low allophycocyanin FRL-PS II samples which contributes to

uncertainties in determining the CD of the broader FRL-chl Q_y excitons. However, both the sign and magnitude of CD for each of the three narrow FRL-chl Q_y peaks remains well determined. This is considered in detail in SI-3. A graphical presentation of the individual CD components, as seen for the MCD components in Fig. 3 is given in Fig S4.

3.4 Analysis of *Electrochromic Shifts*

Illumination of PS II core complexes at cryogenic temperatures induces metastable spectral shifts. Prominent shifts are attributed to the formation of $Q_A^{\bullet-}$. This radical anion is adjacent to $Pheo_{D1}$ and close to Chl_{D1}. It induces relatively large electrochromic shifts of the Q_x band of $Pheo_{D1}$ (historically named the C550 shift) [35] and of the Q_y band of Chl_{D1} [23, 36, 37]. Fig. 4 shows both absorption and illumination difference spectra for a FRL-PS II sample.

These spectra are interpretable in terms of previous analyses of PS II core complex electrochromism [23, 37]. A comparison of representative electrochromism spectra in PS II core complexes of 4 organisms is shown in Fig. S5. In FRL-PS II the C550 shift of the $Pheo_{D1}$ Q_x feature at 544.5 nm is close to the position in other cyanobacterial PS II systems [23]. In some FRL-PSII preparations (SI, Fig S5) a bleach upon photoreduction of Q_A identifies (the initially reduced) cytb$_{559}$ absorption in FRL-PSII to be at 556.5 nm. The dominant blue-shift of Q_y, seen at 1.8 K near 683 nm for *chl-a*-PS II [17, 38] now appears near 726 nm under similar conditions, as reported earlier [1]. This is consistent with the 726 nm band being associated with the primary donor. In *chl-a*-PS II, the Q_y electrochromic shift pattern is dominated by the $Pheo_{D1}$ and Chl_{D1} excitons. The site-energies of the Chl_{D1} and $Pheo_{D1}$ pigments are similar and there is a significant exciton matrix element between them (Table S3). When pigment excitations are close in energy, this matrix element leads them to interact strongly, with intensity being transferred between the resulting excitations [23]. Calculation of the electrochromism requires independent exciton computations of both Q_A and $Q_A^{\bullet-}$ configurations of PS II. Electrochromic effects displace site energies significantly, causing the mixing of exciton states to change. The situation with FRL-PS II is different, as the primary donor is displaced to lower energy by ~ 800 cm^{-1} or more from the *chl-a* excitations. Thus, the effects of the coupling matrix

elements between the primary donor and spatially adjacent pigments such as $Pheo_{D1}$ and P_{D1} are reduced by the energy differences between them, although the matrix elements themselves do not change.
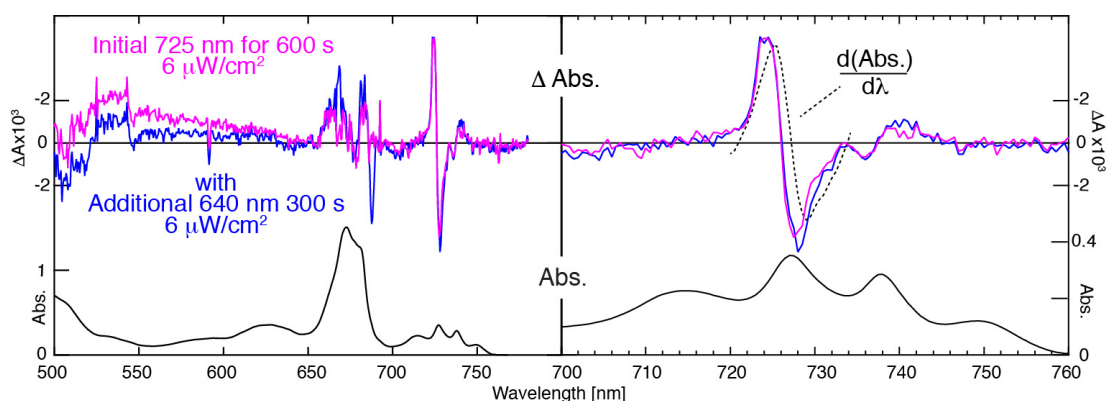

Fig. 4 Lower left panel: 1.8 K absorption spectrum (black line). Upper left panel: Difference spectra after 1. illumination at 725 nm for 600 s with an incident fluence of 6 μW/cm (magenta line), and 2. the total change in absorption induced by the first illumination plus additional illumination at 640 nm (blue line). Right panel: Long-wavelength detail of the absorption and difference spectra shown in the left-hand panels compared to the (scaled) differential of the absorption spectrum taken before illumination (dashed line). This data is analyzed in more detail in SI-4 and Fig. S6.

The spectral isolation of the primary donor Q_y absorption in FRL-PS II assists in the estimation of both its electrochromic shift and the yield of Q_A^- formation. The observed shift appears as a significant fraction of the linewidth and the absorption difference spectrum does not cross precisely at the maximum of absorption (Fig. 4) as would be the case for electrochromic shifts much smaller than the linewidth. The analysis is presented in SI-4 and leads to a yield of 5.5 ± 0.5 % and an initial estimate of the shift at 42 ± 4 cm^{-1}.

However, a quantitative comparison of electrochromic shift data accumulated at 77 K and 1.8 K data taken at higher fluences with low fluence 1.8 K data (Fig. 2), point to a shift magnitude of 42 cm^{-1} to be an overestimate. Instead, it seems that the pigments that photoconvert with high efficiency are only a subset of the total pigment population absorbing at 726 nm. The subset is part of the inhomogeneous distribution of the primary donor excitation energies and this subset is *narrower* than the total distribution and also *shifted* (by ~1 nm) from the peak maximum measured in absorption. The complete analysis is presented in SI-4 and provides a value for the electrochromic shift of 21 ± 4 cm^{-1}.

There is no observable electrochromic shift of the lowest energy feature at 749 nm. The narrow negative feature peaking at 687.5 nm seen in Fig. 4 is not induced by illumination at 725 nm but only with higher energy (640 nm) illumination. This feature is attributed to electrochromism of $chl\text{-}a$-PS II present in the FRL-PS II sample as a contaminant. The data in Fig. 2 and Fig. 4, along with the discussion in SI-4 establish that low power 725 nm illumination does not induce significant $chl\text{-}a$-PS II photochemistry, i.e. does not induce $Q_A^{\bullet-}$ formation as measured by the characteristic Chl_{D1} electrochromic shift in the 685 nm region.

There is a smaller red shift of $\sim 7 \pm 2$ cm^{-1} for the 738 nm peak. This feature is not present at the lowest illumination fluences, see Fig. 2. and Fig. S6. There are also shoulders near the main shift feature that become more pronounced at higher fluences. These may be attributed to secondary photophysical and photochemical processes of the type that also occur in $chl\text{-}a$-PS II and related systems (see SI-4).

The yield of $Q_A^{\bullet-}$ compared to that seen for most other organisms remains low even at high fluences (see SI-4, Fig. S5). However, yields are also very low in *Acaryochloris marina* [39], a system in which PS II is dominated by the FRL-chl $chl\text{-}d$. Strong illumination of FRL-PS II (SI-4, Fig. S6) leads to increased yields, but also induces additional photochemical and photophysical changes [17].

3.5 *Exciton Calculations*

The first widely accepted multi-spectral model [40] for the reaction center of $chl\text{-}a$-PS II used a range of spectral data as input. Exciton couplings between pigments were based on the crystallographically determined distances between chlorins and also the relative orientation of their transition dipoles. A range of exciton realizations were generated to account for the non-correlated inhomogeneity of pigment site-energies. Inhomogeneous widths were seen to be comparable to exciton coupling energies. The authors used a Redfield model for coupled Brownian oscillators to account for temperature dependent data. A simplified version of this model [23], restricted to the analysis of low temperature data, was used to calculate the absorption, CD and electrochromic shifts of the intact reaction center within PS II core complexes in a range of organisms. In this work [23], calculations of electrochromic shifts as well as CD changes associated with both $Q_A^{\bullet-}$ formation and $Pheo_{D1}$ reduction were made.

In the current work, the simplified model [23] is adapted to model the FRL-PS II reaction center absorption spectra, CD and electrochromic shifts. An important point is that the FRL-PS II protein structure, all pigment coupling matrix elements, transition dipoles as well as changes in ground and excited state static dipoles were taken to be the same as those determined by previous studies of *chl-a*-PS II. This is because the crystal structure of FRL-chl has not yet been determined nor has the precise location of the 4 *chl-f's* and 1 *chl-d* pigments.

As a first step, the previously reported analysis [23] of the $Q_A^{\bullet-}$-induced Q_y electrochromic shift pattern, as calculated for plant PS II core complexes at 1.7 K [17], was reproduced and refined (left panel of Fig 5). Then, using the same model, the essential features of the experimental electrochromic pattern in FRL-PS II were reproduced. This model does not take into account i) electrochromic shifts from the low quantum yield side-pathway of electron transfer, including ChlZ bleaching near 670 nm [37], and ii) photophysical shifts of the lowest energy states of CP47 [24] and CP43 [34] near 690 nm. The lowest excited states [41] of peripheral antennae are long-lived and prone to non-resonant hole-burning upon sustained illumination. This last process leads to a redistribution of inhomogeneously distributed pigment site energies to higher energies and in particular, to a reduction of absorption intensity in the lowest energy 690 nm to 700 nm region of spinach PS II, as seen in Fig. 5.

The amplitude of the $Q_A^{\bullet-}$ induced electrochromism reported in spinach PS II core complexes [17], as reproduced in Fig. 5, was that for a $Q_A^{\bullet-}$ yield measured as ~85%. The knowledge of both the yield and amplitude allows an independent and experimental determination of the value of $\Delta\mu/f$, where $\Delta\mu$ is the change in static electric dipole moment between the ground and excited state and f is the dielectric correction factor. Using the previous [42, 43] value of $\Delta\mu$= 1.8 D for *chl-a* and 1.35 D for *pheo-a*, and taking f = 3, as used earlier [23], an excellent fit to the reported [17] spinach PS II shift amplitude near 685 nm is obtained, as shown in Fig. 5. This confirms the use of a value of f=3.
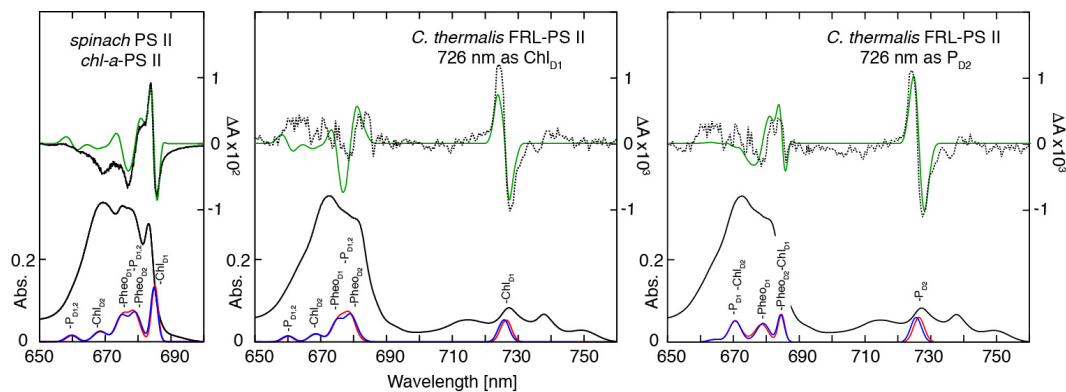
Fig 5. *Lower black traces are absorption spectra of spinach chl-a-PS II core complexes [17] (left panel) and FRL-PS II (center and right panels) at 1.8 K. The upper black traces are experimental electrochromic difference spectra, for 85 % conversion of Q_A to $Q_A^{\bullet-}$ for spinach and ~8% conversion for FRL-PS II (See SI-3). The corresponding green curves are the modelled electrochromism spectra for spinach core complexes (left panel) and FRL-PS II using the Chl_{D1} or P_{D2} options for the location of the 726 nm pigment. The lower red and blue curves are the corresponding calculated absorption spectra of the 6 inner reaction center chlorins for the Q_A and $Q_A^{\bullet-}$ configurations respectively. The upper green traces show the calculated electrochromism. Site energies and the exciton coupling matrix used are given in the Tables S2 and S3.*

The values of $\Delta\mu$=1.8 D for *chl-a* and 1.35 D for *pheo-a* with f = 3 used to fit spinach PS II were used to model FRL-PS II. Except for the FRL 726 nm pigment, for which the position and linewidth was taken from Table S1, site energies and widths of the other (*chl-a*) pigments were left unchanged. The calculations shown in Fig. 5 show that with a (single) FRL-chl placed in the reaction center, either at the Chl_{D1} or P_{D2} position, a strongly blue shifted FRL-PS II electrochromic feature appears (see also Fig. S9). Placing more than one FRL-chl in the reaction center leads to a number of prominent shift features in the far-red region of the electrochromic pattern. Only one prominent shift feature is seen in the low fluence spectra (Fig. 4, Fig. 5). This provides evidence that there is only one FRL-chl in the reaction center. This more detailed treatment confirms the interpretation in the original study [1].

When comparing the calculated electrochromic shift spectra with Chl_{D1} or alternatively P_{D2} as the primary donor against experimental data (Fig. 5), both options reproduce the sign and amplitude of the shift seen at 726 nm. The P_{D2} option provides a somewhat better overall fit to the electrochromic pattern in the *chl-a* Q_y region from 650 nm to 690 nm. FRL PS II data in this region suffers from low signal-to-noise due to i) the higher absorbance present in the *chl-a* Q_y spectral region, ii) the requirement of minimal actinic light and iii) the relatively low yield of $Q_A^{\bullet-}$ formation in FRL-PS II (see Fig. S6) compared to spinach *chl-a*-PS II.

The calculated amplitude of the 726 nm $Q_A^{\bullet-}$ shift is slightly smaller for the Chl_{D1} primary donor case than is for the P_{D2} case, despite P_{D2} being further away (2.6 nm vs 2.2 nm) from Q_A. This is a consequence of the orientation of the electric field with respect to $\Delta\mu$ leading to a larger site-energy shift for P_{D2} (Table S4). The chlorin Q_y site energy shifts for $Q_A^{\bullet-}$ formation (Table S4) shows that the P_{D1} and P_{D2} shifts (5.8 cm^{-1} and 18 cm^{-1}) are comparable to the Chl_{D1} shift (14.4 cm^{-1}).

Exciton modelling can be used to simultaneously calculate the lineshape and amplitude of both CD and absorption spectra [26, 33] without the introduction of any additional parameters. The amplitude of the CD calculated in this way provides a useful internal check of exciton calculations. For the isolated reaction center preparation RC-6 both absorption and CD line-shapes have been successfully modelled [40]. A quantitative comparison of CD and absorption amplitudes was not made at that time. A detailed comparison of more recent, simultaneously taken, lower-temperature absorption and CD spectra, of both RC-6 and RC-5 [26] show that the calculated CD line-shape as well as amplitude are in agreement with the exciton calculations. The calculations done for RC-6 and RC-5 use the same exciton matrix elements (Table S3) as those used here. The only difference in the former calculations were that the linewidths and site-energies introduced were adapted to take into account the increased line-broadening and site-energy blue shifts present in isolated reaction centers such as RC-6, compared to PS II core complexes.

Isolated FRL-PSII reaction centers have not yet been prepared. Consequently, it is only possible to compare theoretical and experimental CD data for the single FRL-chl present in the reaction center component of the FRL-PS II core complex assembly, i.e. the pigment absorbing at 726 nm. The CD characteristics of the other *chl-a* and *pheo-a* FRL-PS II reaction center pigments, i.e. those absorbing in the 650 nm to 690 nm region, are obscured by the dominating CD of *chl-a* present in CP43 and CP47 peripheral antennas (Fig. 1). A more complete analysis would look to calculate the exciton CD of the entire FRL-PS II core assembly but this is not at present feasible. Exciton CD calculations that are restricted to the reaction center pigments of FRL-PS II are a reasonable starting point as couplings between reaction center pigments and pigments in the CP43 and CP47 peripheral antennae are inherently weaker than the

(relatively strong) couplings between reaction centre pigments (Table S3). This is due to the greater inter-

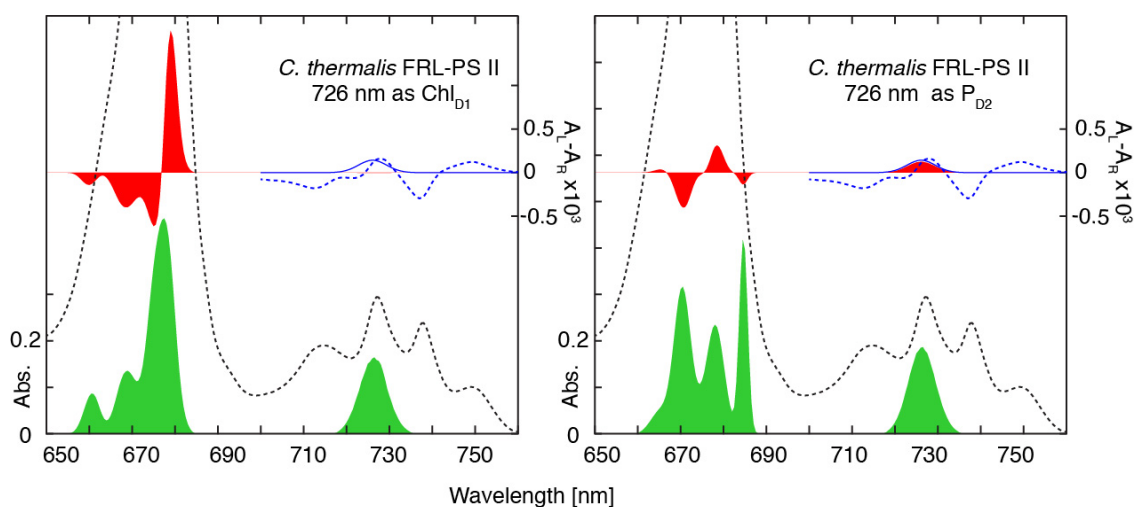pigment distances involved.

Fig 6. For both panels, the dashed black trace (left-hand scale) is the 1.8 K absorption spectrum of a FRL-PS II preparation. The dashed blue trace is the simultaneously-recorded CD spectrum in the red region (right-hand scale). The solid green profiles are the exciton-modelled absorption spectra (see text) of the inner reaction center chlorins of FRL-PS II and the red profiles are the corresponding calculated CD spectra, with either Chl_{D1} or P_{D2} as the primary donor as indicated. The solid blue trace shows the CD component of the primary donor at 726 nm. The position, width and amplitude of the primary donor CD at 726 nm (Table S1) was determined by the global fitting procedure described in the text. Experimental FRL-PS II absorption and CD spectra are scaled to the calculated (reaction center only) spectra by assuming that the integrated absorption area over the entire Q_y region corresponds to a total of ~35 chl and 2 pheo-a pigments with the reaction center having 6 chl and 2 pheo-a pigments. Integrals are shown in Fig S1.

Fig. 6 demonstrates that the computed absorption and CD spectra of the 6 reaction center chlorins in FRL-

PS II, shown as coloured green and red profiles respectively, vary significantly depending on whether the

primary donor is located at Chl_{D1} or P_{D2}. Of the 6 reaction center chlorins, only the FRL-chl primary donor

is directly accessible experimentally, because it has CD and absorption features that are not buried under

the absorption peak arising from ~30 *chl-a* and *2 pheo*-a pigments in the 650 nm - 690 nm region.

The sign and amplitude of the calculated primary donor CD agrees well with the (positive) experimental

CD value when P_{D2} is the primary donor. When Chl_{D1} is the primary donor, the calculated CD is barely

visible. It is 30x smaller and is calculated to have a negative sign. The CD spectrum of a multi-

chromophore array such as a PS II reaction center arises from a complex interplay between exciton

coupling matrix elements (Table S3), site energies (Table S2) and relative orientations of transition dipoles

of the interacting chromophores. Thus, it may not be immediately interpretable. However, there is only one FRL-chl in the reaction center of FRL-PS II (i.e. the pigment at 726 nm) and the Q_y of this pigment is displaced by ~1000 cm^{-1} from the other pigments (*chl-a* and *pheo-a*) in the reaction center. This displacement is larger than the values of the exciton coupling matrix elements shown in Table S3. With coupling matrix elements and orientations being held constant, a large red-shift of the chromophore will tend to have the effect of reducing its CD, whether it be located at Chl_{D1} or P_{D2}.

A quantitative measure of the strength of CD is the parameter ρ_A, the ratio of CD amplitude to absorption, $\Delta A/A$. The CD of the *Chl-a* exciton region at 680 nm in RC-6 is experimental and theoretically evaluated as $\rho_A = 1.2 \times 10^{-3}$. This ρ_A value is significantly less than the calculated CD of the Chl_{D1} exciton itself which has $\rho_A = 2.5 \times 10^{-3}$ [26]. The reduction in ρ_A is due to the significant overlap of the Chl_{D1} exciton with nearby excitons having the opposite CD sign. In FRL-PS II the primary donor exciton is well separated from other reaction center excitons and such cancelling does not occur. Thus, we can directly compare the experimental ρ_A of the primary donor in FRL-PS II with the calculated value of $\rho_A = 2.5 \times 10^{-3}$ for the Chl_{D1} exciton in *chl-a*-PS II.

From our global analysis of FRL-PS II data, the CD of the primary donor in FRL-PS II at 726 nm has $\rho_A = 0.5 \times 10^{-3}$. The calculated values for the primary donor CD $\Delta A/A$ at 726 nm is $\rho_A = 0.6 \times 10^{-3}$ when P_{D2} is the primary donor and -0.02×10^{-3} when Chl_{D1} is the primary donor. In both cases, the calculated ρ_A for the primary donor is far less than the value of $\rho_A = 2.5 \times 10^{-3}$ for the Chl_{D1} exciton in *chl-a*-PS II. A significant reduction in CD for the single FRL-chl in FRL-PS II can be expected regardless of where it is located. This is due to the relatively large energetic difference between the 5 *chl-a* pigments and the single FRL-chl in the reaction center (compared to the coupling matrix elements) reducing the ability of (unchanged) exciton coupling matrix elements to induce CD. The calculated value of $\rho_A = -0.02 \times 10^{-3}$ for the primary donor as Chl_{D1} may appear to be anomalously small given the significant exciton matrix elements between Chl_{D1} and P_{D1}, P_{D2} and $Pheo_{D1}$ (Table S4). This result highlights the fact that the CD of an exciton coupled multi-pigment array is not simply reducible to sums of individual couplings.

Preliminary calculations were performed to explore the influence of proximal antenna-based FRL-chls on

the CD in the 726 nm region. The closest pigment to Chl_{D1} present in CP43, measured edge to edge, is the

'linker' Chl508 [44]. Exciton coupling matrix elements between the reaction center pigments and Chl508

were calculated using a point-dipole approximation [42]. The largest matrix elements between Chl508 and

the reaction center pigments were in the range of 1 cm^{-1} to 7 cm^{-1} and significantly smaller than the largest

matrix elements within the reaction center (Table S3). Exciton CD calculations were then performed for

both the Chl_{D1} and P_{D2} options for the 726 nm pigment, whilst taking Chl508 to be the FRL-chl at 737 nm

(Table S1). The CD calculated at 726 nm when the primary donor was Chl_{D1} became significant in

magnitude but remained negative having $\rho_A = -0.32 \times 10^{-3}$. With P_{D2} as the primary donor, the calculated

CD including Chl508 remained positive with $\rho_A = 0.36 \times 10^{-3}$ and close to the experimental value of

0.47×10^{-3}. In both cases, the sign of the CD calculated for the 737 nm band was positive and thus not in

agreement with experiment (see Fig. 6, Table S1 and Fig. S4). An analogous calculation was made placing

an FRL-chl at the Chl505 location. This is the closest CP43 pigment to Chl_{D1}, measured center to center.

Although the calculated exciton interaction between Chl_{D1} and Chl505 is larger than for Chl508, the CD

with Chl_{D1} is the primary donor is calculated to be significantly smaller than for the Chl508 case described

above and again not in agreement with experiment. A more complete calculation, involving all the

pigments FRL-PS II may help identify the location of the proximal antenna FRL-chls.

In addition to exciton CD, there is the monomeric CD component of *chl* Q_y transitions. This is independent

of, and additive to, exciton CD. Monomeric Q_y CD of *chl-a* is ρ_A -0.16 x 10^{-3} [45], -0.07 x 10^{-3} for *chl-d*

[39] and -0.03 x 10^{-3} for *chl-f* [46]. These values are all small in magnitude and of the opposite sign to the

observed value of $\rho_A = 0.47 \times 10^{-3}$ for the 726 nm band in FRL-PS II.

3.6 *Arguments in favor of the primary donor being Chl_{D1}*
Chl_{D1} is considered to be the primary donor in *chl-a*-PS II [3, 5, 7, 47, 48]. Chl_{D1} is then the obvious

pigment to exchange for a long wavelength pigment [1] to create a low energy primary donor. This

apparently straightforward option is reinforced by the fact that all known FRL-PS II systems for which

sequences are available show a pair of conserved amino acid changes D1Tyr120 and D1Thr155. These can

be modelled as providing H-bonds to the extra formyl group that is the substituent on ring I of the chlorophyll that is responsible for the long-wavelength shift in a FRL-chl [1]. This seems to be a genetic/structural "smoking gun". In contrast, amino acid residues facing the same position in the ring I of P_{D2} appear to be unable to form H-bonds having aliphatic side chains (Val and Leu). These residues were also found to be conserved in both the FRL and WL version of PSII. Nevertheless, we cannot exclude H-bond formation via the amide group of the peptide bond.

The mechanistic and redox arguments cited in the introduction are also strong. Given the similar rates and efficiency of O_2 evolution, it is assumed that the donor-side components of FRL PS II are tuned to have the same redox potentials as in chl-a-PS II [1]. Thus, the primary electron donor FRL- chl$^{•+}$/chl is taken as having a similar potential as its counterpart in chl-a-PSII. However, FRL-chl absorbing at 725nm will have ~110 meV less energy available in the excited state than does chl-a absorbing at ~680nm. This will result in the FRL-chl$^{•+}$/chl* couple having higher potentials and therefore FRL-chl* will have less reducing power than its chl-a counterpart [1].

A less reducing FRL-chl* strongly favors pheo-a as the primary electron acceptor because the pheo-a/pheo-a$^{•-}$ couple has a much higher reduction potential than that of chl-a/chl-$a$$^{•-}$. The structure dictates that Pheo-a can only be the primary acceptor when Chl$_{D1}$* is the primary donor and this provides a good argument for the primary donor being Chl$_{D1}$ in FRL-PS II [1]. In models in which P_{D2} is the primary donor, the primary acceptor would be chl-a (either P_{D1} or Chl$_{D1}$). This is expected to be unfavorable in redox terms. A similar argument was made for assigning the chl-d primary donor on Chl$_{D1}$ in $Acaryochloris\ marina$ PS II [4]. Along the same lines, recent calculations of the redox potentials of the chlorins in chl-a-PSII indicated that Chl$_{D1}$* electron donation to Pheo$_{D1}$ is favorable, but that P_{D1}* donation to Chl$_{D1}$ is energetically unfavorable [48]. If this trend is extrapolated to FRL-PSII, FRL-chl* is expected to be even less capable of reducing a chl-a primary acceptor.

The chemical argument mentioned in the introduction comes from the demonstration that chlorophyll has acid base properties that will favor ligation to water over histidine [49]. In the chl-a-PS II reaction center, only the Chl$_{D1}$ and Chl$_{D2}$ pigments have water coordination and are thus more likely as candidates for

replacement by *chl-f* [1]. It is not possible to rule out histidine ligation to *chl-f*, in either the PS II reaction center or in peripheral antenna, but the chemical preference exists.

4. Conclusions

Illumination of FRL-PS II at 1.8 K at a series of wavelengths confirmed that the pigment at 726 nm is the primary electron donor. Charge separation occurred relatively efficiently at wavelengths ≤ 726 nm but became much less efficient at longer wavelengths. This verifies the conclusion made earlier [1].

A global analysis of absorption, CD and MCD data enabled the determination of the exciton spectral amplitudes, positions and widths of all 5 FRL-chl Q_y state spectral components in FRL-PS II. The $Q_A^{\bullet-}$ induced electrochromism in FRL-PS II generated by low temperature and low fluence illumination was modelled by exciton coupling calculations (Figs. 5, 6 and S9). The starting point for these calculations was a new *quantitative* analysis of existing electrochromism data of *chl-a*-PS II core complexes prepared from spinach, allowing a model-free determination of the value of $\Delta\mu/f$. The FRL-PS II electrochromic shift at 726 nm could be quantitatively accounted for by transferring the Chl_{D1} or P_{D2} *chl-a* site energy appropriate to spinach to the FRL 726 nm position, whilst leaving all exciton coupling terms, other site energies and geometric parameters as well as $\Delta\mu/f$ unchanged. The P_{D2} calculation provided a slightly better fit to the overall electrochromic pattern in the 650 nm to 690 nm region. The exciton modelling was also able to exclude the possibility that there was more than one FRL-chl in the reaction center, again in line with earlier ideas [1].

The CD calculated by the exciton modelling was able to account for the observed value of $\rho_A =\Delta A/A$ at 726 nm, without the use of additional parameters, when the primary donor was located at P_{D2}. When located at Chl_{D1} the CD calculated was 30 times smaller and of the wrong sign in comparison to experiment. Preliminary exciton calculations of coupling between the reaction center chlorins and the closest chlorins in the proximal antennas (Chl508 and Chl505) indicate that coupling an FRL-chl at either of these locations are unlikely to account for the experimentally observed CD amplitude at 726 nm. A more definitive calculation would be to include all the pigments in FRL-PS II or perhaps a subset of the CP43 and CP47

pigments closest to the reaction center pigments. Such calculations may help identify the location of the FRL-chls in the proximal antennae.

There are a number of arguments that make a good case for the Chl_{D1} being the location of the single FRL-chl in the reaction center. However, these arguments are intuitive, mechanistic and, when structural (i.e. the conserved amino acid changes) are yet to be verified by experiment. The current work presents initial experimental evidence, particularly from the concurrence of calculated and experimental CD at 726 nm, that the primary donor could be located at P_{D2}.

Rather than speculating further on this surprising result, we look to perform additional spectroscopic experiments and calculations that may provide further evidence relevant to the character and location of the primary donor in FRL-PS II.

Acknowledgements

References

[1] D.J. Nurnberg, J. Morton, S. Santabarbara, A. Telfer, P. Joliot, L.A. Antonaru, A.V. Ruban, T. Cardona, E. Krausz, A. Boussac, A. Fantuzzi, A.W. Rutherford, Photochemistry beyond the red limit in chlorophyll f-containing photosystems, Science, 360 (2018) 1210-1213.

[2] T. Renger, E. Schlodder, The primary electron donor of photosystem II of the cyanobacterium Acaryochloris marina is a chlorophyll d and the water oxidation is driven by a chlorophyll a/chlorophyll d heterodimer, Journal of Physical Chemistry B, 112 (2008) 7351-7354.

[3] T. Cardona, A. Sedoud, N. Cox, A.W. Rutherford, Charge separation in Photosystem II: A comparative and evolutionary overview, Bba-Bioenergetics, 1817 (2012) 26-43.

[4] T. Renger, E. Schlodder, Optical properties, excitation energy and primary charge transfer in photosystem II: Theory meets experiment, J Photoch Photobio B, 104 (2011) 126-141.

[5] B.A. Diner, F. Rappaport, Structure, Dynamics, and Energetics of the Primary Photochemistry of Photosystem II of Oxygenic Photosynthesis, Annu Rev Plant Biol., 53 (2002) 551-580.

[6] A.R. Holzwarth, M.G. Muller, M. Reus, M. Nowaczyk, J. Sander, M. Rogner, Kinetics and mechanism of electron transfer in intact photosystem II and in the isolated reaction center: Pheophytin is the primary

electron acceptor, Proceedings of the National Academy of Sciences of the United States of America, 103 (2006) 6895-6900.

[7] E. Romero, I.H.M. van Stokkum, V.I. Novoderezhkin, J.P. Dekker, R. van Grondelle, Two Different Charge Separation Pathways in Photosystem II, Biochemistry, 49 (2010) 4300-4307.

[8] J.K. Hoober, L.L. Eggink, M. Chen, Chlorophylls, ligands and assembly of light-harvesting complexes in chloroplasts, Photosynthesis Research, 94 (2007) 387-400.

[9] S.A. Masami Kobayashi, Daiki Fujinuma, Hayato, H.K. Furukawa, Yuichi Hotota, Yuki Kato, Yoshinori, T.W. Kuroiwa, Mayumi Ohnishi-Kameyama, Hiroshi, S.O.a.H.M. Ono, Physicochemical Properties of Chlorophylls in Oxygenic Photosynthesis — Succession of Co-Factors from Anoxygenic to Oxygenic Photosynthesis, IntechOpen, 2013.

[10] F. Muh, M. Plockinger, T. Renger, Electrostatic Asymmetry in the Reaction Center of Photosystem II, J Phys Chem Lett, 8 (2017) 850-858.

[11] E.W. Knapp, S.F. Fischer, W. Zinth, M. Sander, W. Kaiser, J. Deisenhofer, H. Michel, Analysis of Optical-Spectra from Single-Crystals of Rhodopseudomonas-Viridis Reaction Centers, Proceedings of the National Academy of Sciences of the United States of America, 82 (1985) 8463-8467.

[12] T. Wydrzynski, K. Satoh, Photosystem II - The Light-Driven Water:Plastoquinone Oxidoreductase in: Govindjee (series ed), Advances in Photosynthesis and Respiration Vol. 22 pp 786. Springer, Dordrecht, The Netherlands., 2005.

[13] R. Steffen, J. Hughes, P. Smith, R. Pace, A. Rutherford, E. Krausz, Secondary donors in low-temperature optical spectroscopy of photosystem II, Photosynthesis Research, 91 (2007) 147-147.

[14] E. Krausz, Selective and Differential Optical Spectroscopies in Photosynthesis, Photosynthesis Research, (2013).

[15] J. Morton, F. Akita, Y. Nakajima, J.-R. Shen, E. Krausz, Optical identification of the long-wavelength (700–1700nm) electronic excitations of the native reaction centre, Mn4CaO5 cluster and cytochromes of photosystem II in plants and cyanobacteria, Biochimica et Biophysica Acta (BBA) - Bioenergetics, 1847 (2015) 153-161.

[16] J. Morton, M. Chrysina, V.S.J. Craig, F. Akita, Y. Nakajima, W. Lubitz, N. Cox, J.R. Shen, E. Krausz, Structured near-infrared Magnetic Circular Dichroism spectra of the Mn4CaO5 cluster of PSII in T. vulcanus are dominated by Mn(IV) d-d 'spin-flip' transitions, Bba-Bioenergetics, 1859 (2018) 88-98.

[17] J.L. Hughes, P. Smith, R. Pace, E. Krausz, Charge Separation in Photosystem II Core Complexes Induced by 690-730 nm Excitation at 1.7 K, Biochimica et Biophysica Acta, 1757 (2006) 841-851.

[18] P.J. Smith, S. Peterson, V.M. Masters, T. Wydrzynski, S. Styring, E. Krausz, R.J. Pace, Magneto-Optical Measurements of the Pigments in Fully Active Photosystem II Core Complexes from Plants, Biochemistry, 41 (2002) 1981-1989.

[19] S. Peterson Årsköld, V.M. Masters, B.J. Prince, P.J. Smith, R.J. Pace, E. Krausz, Optical Spectra of Synechocystis and Spinach Photosystem II Preparations at 1.7 K: Identification of the D1-Pheophytin Energies and Stark Shifts, Journal of the American Chemical Society, 125 (2003) 13063-13074.

[20] J. Morton, J. Hall, P. Smith, F. Akita, F.H. Koua, J.R. Shen, E. Krausz, Determination of the PS I content of PS II core preparations using selective emission: a new emission of PS II at 780nm, Biochim Biophys Acta, 1837 (2014) 167-177.

[21] C.A. Tracewell, G.W. Brudvig, Multiple Redox-Active Chlorophylls in the Secondary Electron-Transfer Pathways of Oxygen-Evolving Photosystem II, Biochemistry, 47 (2008) 11559-11572.

[22] H.C. Chang, R. Jankowiak, C.F. Yocum, R. Picorel, M. Alfonso, M. Seibert, G.J. Small, Exciton Level Structure and Dynamics in the CP47 Antenna Complex of Photosystem II, Journal of Physical Chemistry, 98 (1994) 7717-7724.

[23] N. Cox, J.L. Hughes, R. Steffen, P.J. Smith, A.W. Rutherford, R.J. Pace, E. Krausz, Identification of the Q(Y) Excitation of the Primary Electron Acceptor of Photosystem II: CD Determination of Its Coupling Environment, Journal of Physical Chemistry B, 113 (2009) 12364-12374.

[24] J. Hall, T. Renger, F. Muh, R. Picorel, E. Krausz, The lowest-energy chlorophyll of photosystem II is adjacent to the peripheral antenna: Emitting states of CP47 assigned via circularly polarized luminescence, Biochim Biophys Acta, 1857 (2016) 1580-1593.

[25] E. Krausz, J.L. Hughes, P. Smith, R. Pace, S. Peterson Årsköld, Oxygen-Evolving Photosysten II Core Complexes: A New Paradigm Based on the Spectral Identification of the Charge-Separating State, the Primary Acceptor and Assignment of Low-Temperature Fluorescence, Photochemical and Photobiological Sciences, 4 (2005) 744-753.

[26] J. Hall, R. Picorel, N. Cox, R. Purchase, E. Krausz, New Perspectives on Photosystem II Reaction Centres

, Australian Journal of Chemistry, (2020).

[27] S.P. Årsköld, P.J. Smith, J.-R. Shen, R.J. Pace, E. Krausz, Key cofactors of Photosystem II cores from four organisms identified by 1.7-K absorption, CD and MCD, Photosynth. Res., 84 (2005) 309-316.

[28] S.B. Piepho, P.N. Schatz, Group Theory in Spectroscopy with Applications to Magnetic Circular Dichroism, Wiley-Interscience, New York, Chichester, Brisbane, Toronto, Singapore, 1983.

[29] D. Zevenhuijzen, P.J. Zandstra, Absorption and Magnetic Circular Dichroism of Chlorophyll *a* and *b* Dimers, Biophysical Chemistry, 19 (1984) 121-129.

[30] J.L. Hughes, R.J. Pace, E. Krausz, The Exciton Contribution to the Faraday B term MCD of Molecular Dimers, Chemical Physics Letters, 385 (2004) 116-121.

[31] Y.Q. Li, N. Scales, R.E. Blankenship, R.D. Willows, M. Chen, Extinction coefficient for red-shifted chlorophylls: Chlorophyll d and chlorophyll f, Bba-Bioenergetics, 1817 (2012) 1292-1298.

[32] Y.Q. Li, Z.L. Cai, M. Chen, Spectroscopic Properties of Chlorophyll f, Journal of Physical Chemistry B, 117 (2013) 11309-11317.

[33] H. van Amerongen, R. van Grondelle, L. Valkunas, Photosynthetic Excitons, WORLD SCIENTIFIC, 2000.

[34] J. Hall, T. Renger, R. Picorel, E. Krausz, Circularly polarized luminescence spectroscopy reveals low-energy excited states and dynamic localization of vibronic transitions in CP43, Bba-Bioenergetics, 1857 (2016) 115-128.

[35] W.L. Butler, Primary Photochemistry of Photosystem II of Photosynthesis, Accounts of Chemical Research, 6 (1973) 177-184.

[36] D.H. Stewart, P.J. Nixon, B.A. Diner, G.W. Brudvig, Assignment of the Q_y Absorbance Bands of Photosystem II Chromophores by Low-Temperature Optical Spectroscopy of Wild-Type and Mutant Reaction Centres, Biochemistry, 39 (2000) 14583-14594.

[37] E. Schlodder, T. Renger, G. Raszewski, W.J. Coleman, P.J. Nixon, R.O. Cohen, B.A. Diner, Site-directed Mutations at D1-Thr179 of Photosystem II in Synechocystis sp. PCC 6803 Modify the Spectroscopic Properties of the Accessory Chlorophyll in the D1-branch of the Reaction Center, Biochemistry, (2008).

[38] J.L. Hughes, B.J. Prince, E. Krausz, P.J. Smith, R.J. Pace, H. Riesen, Highly Efficient Spectral Hole-Burning in Oxygen-Evolving Photosystem II Preparations, Journal of Physical Chemistry B, 108 (2004) 10428-10439.

[39] M.R. Razeghifard, M. Chen, J.L. Hughes, J. Freeman, E. Krausz, T. Wydrzynski, Spectroscopic Studies of Photosystem II in Chlorophyll *d*-containing *Acaryochloris marina*, Biochemistry, 44 (2005) 11178-11187.

[40] G. Raszewski, W. Saenger, T. Renger, Theory of Optical Spectra of Photosystem II Reaction Centers: Location of the Triplet State and the Identity of the Primary Electron Donor, Biophysical Journal, 88 (2005) 986-998.

[41] J.R. Reimers, M. Biczysko, D. Bruce, D.F. Coker, T.J. Frankcombe, H. Hashimoto, J. Hauer, R. Jankowiak, T. Kramer, J. Linnanto, F. Mamedov, F. Muh, M. Ratsep, T. Renger, S. Styring, J. Wan, Z. Wang, Z.Y. Wang-Otomo, Y.X. Weng, C. Yang, J.P. Zhang, A. Freiberg, E. Krausz, Challenges facing an understanding of the nature of low-energy excited states in photosynthesis, Biochim Biophys Acta, (2016).

[42] G. Raszewski, B.A. Diner, E. Schlodder, T. Renger, Spectroscopic properties of reaction center pigments in photosystem II core complexes: Revision of the multimer model, Biophysical Journal, 95 (2008) 105-119.

[43] V.I. Novoderezhkin, J.P. Dekker, R. van Grondelle, Mixing of Exciton and Charge-Transfer States in Photosystem II Reaction Centers: Modeling of Stark Spectra with Modified Redfield Theory, Biophys. J., 93 (2007) 1293-1311.

[44] Y. Umena, K. Kawakami, J.R. Shen, N. Kamiya, Crystal structure of oxygen-evolving photosystem II at a resolution of 1.9 angstrom, Nature, 473 (2011) 55-U65.

[45] C. Houssier, K. Sauer, Circular Dichriosm and Magnetic Circular Dichroism of the Chlorophyll and Protochlorophyll Pigments, Journal of the American Chemical Society, 92 (1970) 779-791.

[46] R.D. Willows, Y.Q. Li, H. Scheer, M. Chen, Structure of Chlorophyll f, Org Lett, 15 (2013) 1588-1590.

[47] A.R. Holzwarth, M.G. Mueller, M. Reus, M. Nowaczyk, J. Sander, M. Roegner, Kinetics and Mechanism of Electron Transfer in Intact Photosystem II and in the Isolated Reaction Center: Pheophytin is the Primary Electron Acceptor, Proceedings of the National Academy of Sciences of the United States of America, 103 (2006) 6895-6900.

[48] K. Kawashima, H. Ishikita, Energetic insights into two electron transfer pathways in light-driven energy-converting enzymes, Chem Sci, 9 (2018) 4083-4092.

[49] M. Chen, Chlorophyll Modifications and Their Spectral Extension in Oxygenic Photosynthesis, Annual Review of Biochemistry, Vol 83, 83 (2014) 317-340.

Supplementary Information

The primary donor of far-red Photosystem II: Chl_{D1} or P_{D2}?

Martyna Judd[1], Jennifer Morton[1], Dennis Nürnberg[2], Andrea Fantuzzi[2], A. William Rutherford[2],

Robin Purchase[1], Nicholas Cox[1] and Elmars Krausz*[1]

[1] Research School of Chemistry, Australian National University, Canberra 2600, Australia

[2] Department of Life Sciences, Imperial College, London SW7 2AZ, United Kingdom

SI-1 Allophycocyanin and FRL chlorophyll content of FRL-PS II

The quantification of the five far red chlorophylls in FRL-PS II presents a challenge. Fig. 2 of the manuscript identifies the presence of allophycocyanins which overlap the spectral region where the FRL chlorins, *chl-f* and *chl-d*, absorb.
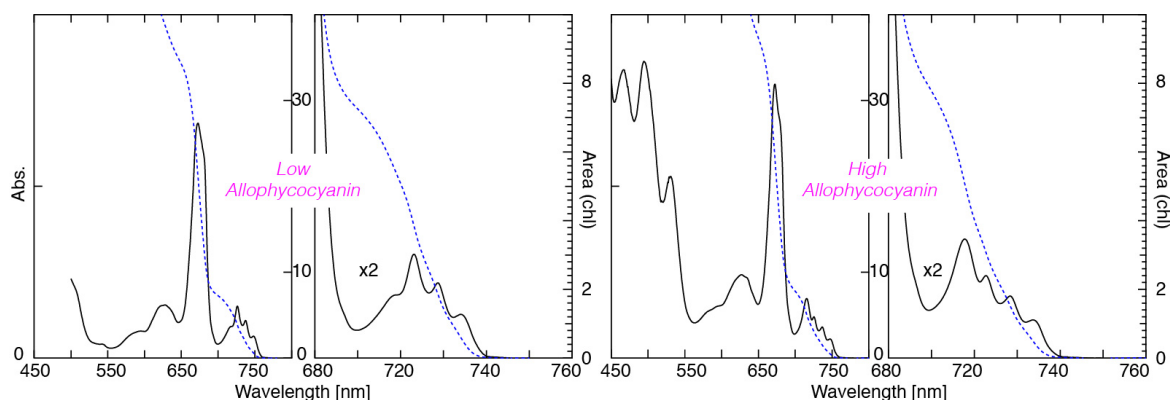

Fig. S1 Absorption spectra of low allophycocyanin and high allophycocyanin FRL-PS II at 1.8 K along with their integrals (dashed curves), scaled to ~35 chl total Q_y absorbance.

Fig. S1 provides the integrals of absorption in the Q_y regions. Both high and low allophycocyanin samples have total absorption in the 700 nm - 800 nm region that exceeds a value corresponding to 5 chls by ~2-3 chl. This result is based on all chls having the same oscillator strength for Q_y which is the approximation proposed in the manuscript. The contamination of FRL-PS II samples with *chl-a*-PS II can be estimated to be ~7% from the

fluorescence measurements provided in Fig. S3 and the ensuing discussion. The level of contamination by *chl-a*-PS II would thus only reduce the estimate of allophycocyanin component of the FRL absorption by this (small) percentage. The molar extinction of allophycocyanins isolated from *Synechocystis* is ~2x10^5 M^{-1} cm^{-1} for both types of allophycocyanin found in this organism. Thus, there are likely to be ~1-2 allophycocyanin per FRL-PS II in our preparations.

Allophycocyanins are known to form both monomers and trimers [1] with trimers being red shifted. This variability precludes a quantitative assessment of the allophycocyanin components. Different monomer and trimer allophycocyanin content is likely to be responsible for the changing spectral profiles in absorption and CD of allophycocyanin components (see Fig. 3 of manuscript).

SI-2 Fluorescence Excitation Spectra and Temperature Dependent Fluorescence

Fig. 1 of the manuscript highlights the difference between the emission spectra of the *chl-a*-PS II and that of FRL-PS II. In the latter the dominant peak is at 752 nm, with a weaker emission in the 720 nm region, attributable to allophycocyanin.
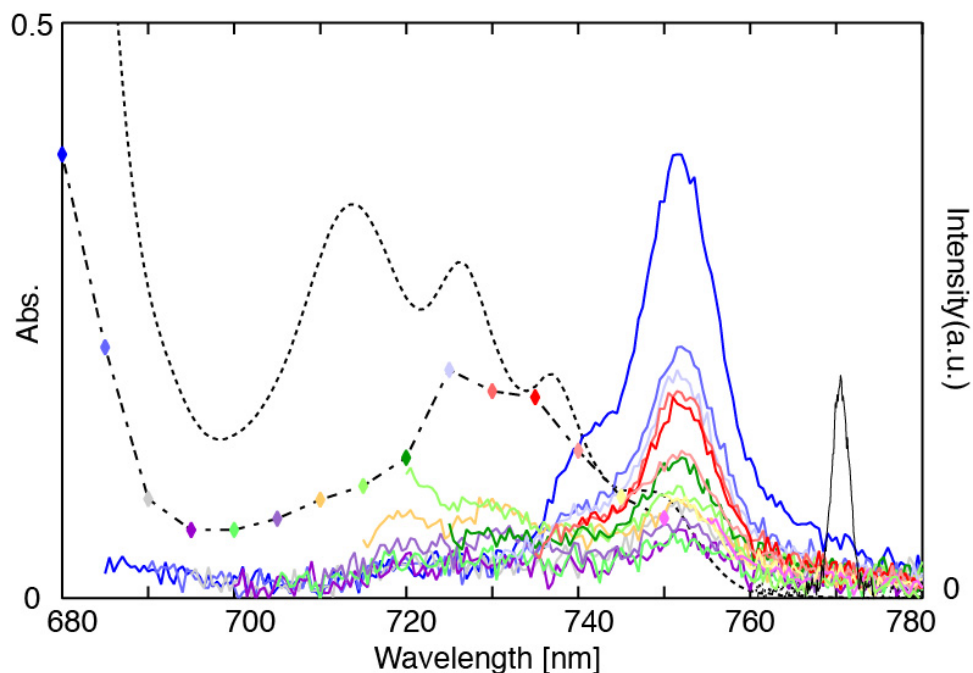
Fig. S2 *The absorption spectrum (dotted line) and the emission spectra (coloured lines) of FRL-PSII are shown. Spectra were taken at 77 K of a high-allophycocyanin FRL-PSII sample. The emission spectra were taken with excitation at different wavelengths in 5 nm steps from 680 nm to 755 nm. The corresponding excitation spectrum (composed of coloured diamonds which are joined by a double-dashed line) is generated by plotting the amplitude of the emission peak at 755 nm. The colour of each diamond in the excitation spectrum matches that of the corresponding emission spectrum. The narrow peak seen at 770 nm (black line) is obtained by measuring 770 nm exciting light. This spectrum serves to calibrate the excitation light bandwidth from the monochromator as ~2.4 nm FWHM.*

The spectra in Fig. S2 show that allophycocyanin absorption leads to a low level of emission from FRL-PS II. The excitation spectrum presented in Fig. S2 is similar to the MCD spectra of FRL-PS II in Fig. 1 of the manuscript in that the characteristic 714 nm allophycocyanin peak is missing. Absorption in the 680 nm to 710 nm region leads to the weaker emission peak at ~720 nm which does not correspond to the 714 nm absorption. This emission likely arises from a form of allophycocyanin (monomer, trimer etc.) present in the sample that is not functionally connected to FRL-PS II (see below).

Fig. S3 shows the excitation dependence of the well-resolved fluorescence in a high-allophycocyanin sample at 1.8 K. The weak emission from the contamination by *chl-a*-PS II in the 685nm – 693 nm region, and an allophycocyanin peak at 720 nm discussed above, are apparent, as well as the double peak feature at 741 nm and 752 nm associated with FRL-PS II. The relative intensities of the double peaks in FRL-PS II (Fig. S3) do not vary with excitation wavelength. This indicates that both peaks originate from the FRL PS II component of the FRL-PS II core complex. Additionally, the intensity of the 720 nm peak, when excited at different wavelengths, does not scale with that of the double peaks, indicating it arises from a allophycocyanin in the FRL-PS II preparation and a further indication that the allophycocyanin does not transfer all its excitation energy to a PS II core assembly.
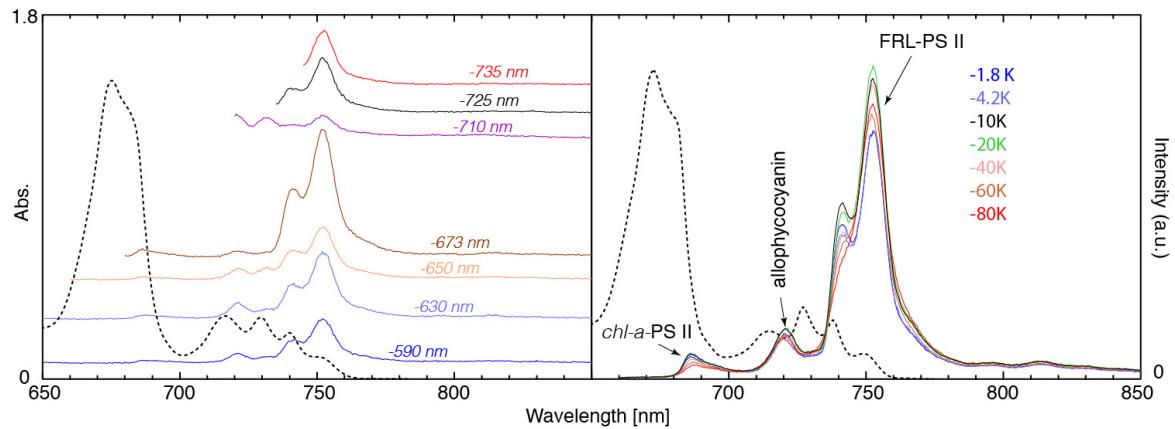
Fig. S3 *Excitation dependence of fluorescence from a high-allophycocyanin FRL-PS II preparation at 1.8 K (left panel). Temperature dependent emission of a medium-allophycocyanin sample excited at 532 nm (right panel). Absorption spectra (black dotted lines) are provided for comparison in both panels.*

The temperature dependence of the high energy fluorescence component in the 680 nm to 700 nm region (Fig. S3) shows the temperature dependence of *chl-a*-PS II [2], which is clearly present as a contaminant in this sample. Assuming PS II core complexes of FRL-PS II and *chl-a*-PS II have comparable quantum efficiencies in emission and have equivalent absorption strengths at the excitation wavelengths used, the contamination level is estimated to be ~7 %. Fig. S3 identifies a modest decrease in the allophycocyanin fluorescence at 720 nm in the 1.8 K to 80 K range. It exhibits a simple broadening in spectral profile. This behavior is typical for an isolated antenna assembly such as CP43 [3] or CP47 [4].

The PS II core complex emission component of FRL-PSII, having emission peaks at 741 nm and 753 nm, shows a stronger and more complex temperature dependence. The two peaks have distinctly different temperature dependence, with the 742 nm peak reducing in amplitude with temperature more quickly than the 753 nm peak. This temperature dependent behavior is reminiscent of that shown by *chl-a*-PS II where the higher energy component can be attributed [2, 5, 6] to CP43 at the lowest temperatures. This peak becomes less prominent at higher temperatures. The barrier to excitation transfer to the reaction center is overcome by thermal

activation at higher temperatures and consequently emission from the lowest energy excitations of CP43 becomes depleted.

SI-3 Determination of the five FRL chlorophyll Q_y Bands

An initial estimation the peak positions and linewidths of the three distinct FRL chlorophyll features is straightforward. There is some indication of a high-energy shoulder near 713 nm in the MCD spectra (see Fig. 3 of the manuscript) and is also visible in the excitation spectrum shown in Fig. S2.

Attempts to fit MCD spectra with five Gaussians, one for each FRL chlorophyll, did not provide a uniquely defined fit. These attempts do indicate that two FRL Q_y absorptions have greater linewidths than the three obvious features. Absorption and CD spectra do not assist greatly in locating the positions and widths of the two remaining FRL chlorophyll molecules, owing to interference by allophycocyanins.

The amplitude of the MCD relative to the absorption (B/D) of chlorins is known to vary significantly [2, 7-10] with the primary donor having a greatly reduced value of B/D. The approach developed was to subtract a scaled absorption spectrum from the corresponding MCD spectrum and vary the scaling factor until each well-resolved FRL chlorophyll feature in the MCD spectrum was nulled. This procedure worked well and provided relative B/D ratios for each of the three distinct FRL chlorophyll Q_y absorptions.

These pre-determined relative B/D ratios were then held constant in a five band Gaussian fitting of the MCD spectrum. This process determined the position, width and relative B/D of the two remaining FRL chlorophylls, i.e. Chl-3 and Chl-5, as shown in Table S1. The same positions, widths and relative B/D values were obtained in independent analyses of both high and low allophycocyanin MCD spectra.

The positions and widths of Chl-3 and Chl-5 were not dependent on the precise value of their relative B/D values (these are proportional to the 'Relative Area MCD' column in Table S1). The best overall fit was obtained when Chl-1, Chl-3 and Chl-5 had equal B/D values. The primary donor (Chl-4) had a smaller B/D value. This is consistent with previous observations of B/D for the primary donor in *chl-a*-PS II [2, 7-10] although the full chemical significance of this notable electronic characteristic of primary donors is not understood.

Having determined the position and width of each FRL chlorophyll Q_y excitation (Table S1), the FRL chlorophyll Q_y absorption spectrum was then fitted to five bands of equal area. This process involved a single linear fitting parameter. Two Gaussians were introduced to account for the allophycocyanins absorptions (allophycocyanin-1 and allophycocyanin-2 in Table S1). The narrow allophycocyanin component (allophycocyanin-1) in high-allophycocyanin and low-allophycocyanin samples are similar but allophycocyanin-2 is quite different. The fits for allophycocycanin-1 and allophycocyanin-2 -shown in Fig 3 of the manuscript and Table S1 remain indicative only, as there is significant correlation between fitting parameters. The presence of different forms of allophycocyanins was discussed in SI-1.

In Table S1 the relative area of the Chl-4 absorption was revised to have a value of 1.1 chl. Exciton modelling (SI-4) establishes that the interactions between the FRL chlorophyll primary donor and its *chl-a* neighbors within the reaction center leads to this (relatively low) level of transfer of intensity.

The CD spectra were then fitted, with the amplitude of each Q_y CD feature allowed to vary. The allophycocyanin CD components were allowed unconstrained amplitudes, widths and positions. The widths and positions of allophycocyanin CD features are not those as determined by the corresponding fit of the absorption spectrum. For the five FRL chlorophyll Q_y excitations, each is an individual exciton Q_y component. The CD profile of a single purely electronic Q_y excitation follows that seen in absorption [11]. The absorption profiles of

allophycocyanins are composite of a number of exciton-coupled pigment excitations. Thus

allophycocyanin CD profiles do not follow those in absorption [1, 12].

Table S1 FRL-PS II Global Analysis

High allophycocyanin sample

Band	Absorption nm & (FWHM) nm	Energy cm^{-1} (Shift$^{\#}$) cm^{-1}	Area Abs.	Area MCD	Area CD
Chl-1	749 (9)	13350 (0)	1	1	1
Chl-2	738 (6)	13550 (200)	1	0.7	-1.4
Chl-3	733 (9)	13640 (310)	1	1	0.3
Chl-4*	726 (6)	13760 (410)	1.1	0.6	0.6
Chl-5	722 (14)	13850 (500)	1	1	0.0
a-1	714 (8)	14010 (660)	1.9	0	-1.5
a-2	708 (25)	14120 (780)	5.3	0	-1.6

Low allophycocyanin sample

Band	Absorption nm (FWHM) nm	Energy cm^{-1} (Shift$^{\#}$) cm^{-1}	Area Abs.	Area MCD	Area CD
Chl-1	748 (10)	13370 (0)	1	1	1
Chl-2	737 (7)	13570 (200)	1	0.7	-1.6
Chl-3	731 (12)	13680 (310)	1	1	0.9
Chl-4*	726 (6)	13770 (410)	1.1	0.6	0.6
Chl-5	720 (15)	13890 (520)	1	1	-1.2
a-1	716 (8)	13970 (630)	0.6	0	-0.7
a-2	705 (14)	14180 (820)	1.2	0	-0.4

Areas are relative to the absorption, MCD or CD areas of Chl-1
$^{\#}$ *Shifts are relative to the peak of Chl-1*
* *Primary donor.*
a-1 - allophycocyanin-1
a-2 - allophycocyanin-2

The right-hand columns in Table S1 show that the area of Q_y CD features associated with Chl-

1, Chl-2 and Chl-4 reproduce well between the high and low allophycocyanin samples,

whereas discrepancies appear for Chl-3 and Chl-5. Fig S4 provides a comparison of the

experimental and fitted CD for high and low allophycocyanin samples, along with the

individual CD components determined by the fitting procedure described above.

A significant discrepancy is that Chl-5 is attributed to have minimal CD in the high

allophycocyanin sample but a strong negative CD in the low allophycocyanin sample. By

contrast, the three sharp FRL-chl features, Chl-1, Chl-2 and Chl-4 are well determined in both samples and their CD amplitudes are not significantly correlated. However, the fit of Chl-3, Chl-5, a-1 and a-2 CD features are significantly correlated, particularly for the low allophycocyanin CD data. The region of major discrepancy (720 nm) shows a sharp inflection in both samples that is not reproduced in either absorption or MCD data. A more complete representation of allophycocyanin CD thus requires extra components in the fitting procedure. Additionally, rather than a simple reduction of allophycocyanin content between the two samples, it seems that extra (allophycocyanin) assemblies are introduced via the procedure used to reduce the total allophycocyanin content. These assemblies appear to have significant negative CD in the 720 nm to 730 nm region, making it impossible to disassociate it from CD associated with Chl-5. Without further experimental information, we cannot determine the CD of Chl-5. It seems likely that the CD of Chl-3 is significant and positive.
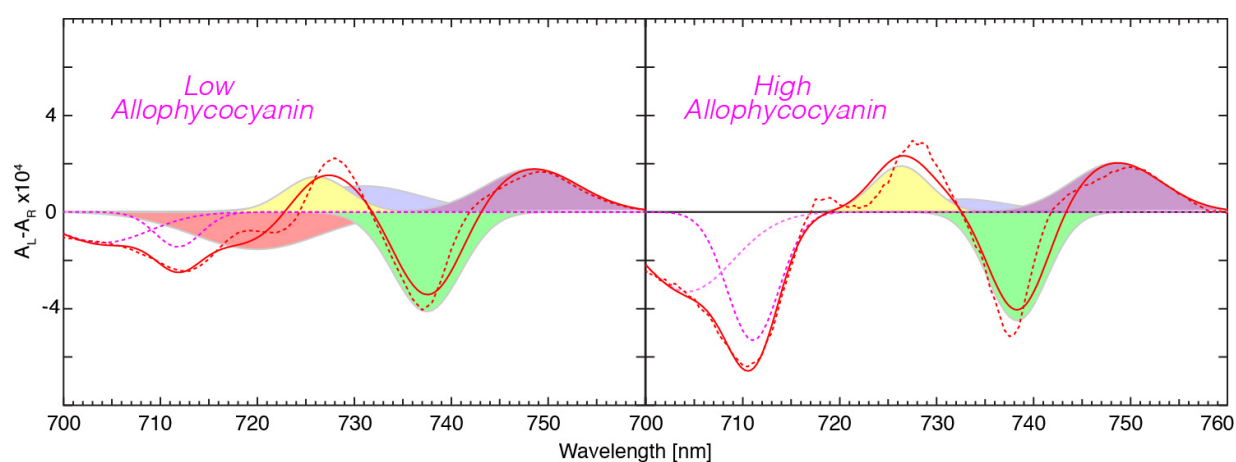

Fig. S4. *The 1.8 K experimental CD and corresponding fitted CD spectra of low and high allophycocyanin FRL-PS II samples are shown as dotted and solid red lines respectively. These spectra are also presented in Fig. 3 of the manuscript in less detail and are displayed in conjunction with corresponding absorption and MCD data and analysis. The fitted CD components (see text) are displayed as coloured overlapping Gaussians using the same colour scheme as used in Fig. 3.*

SI-4 Electrochromic Shifts

A comparison of $Q_A{}^{\bullet-}$ formation-induced electrochromic shift patterns for a range of organisms compared to those seen in FRL-PS II, is provided in Fig S5.
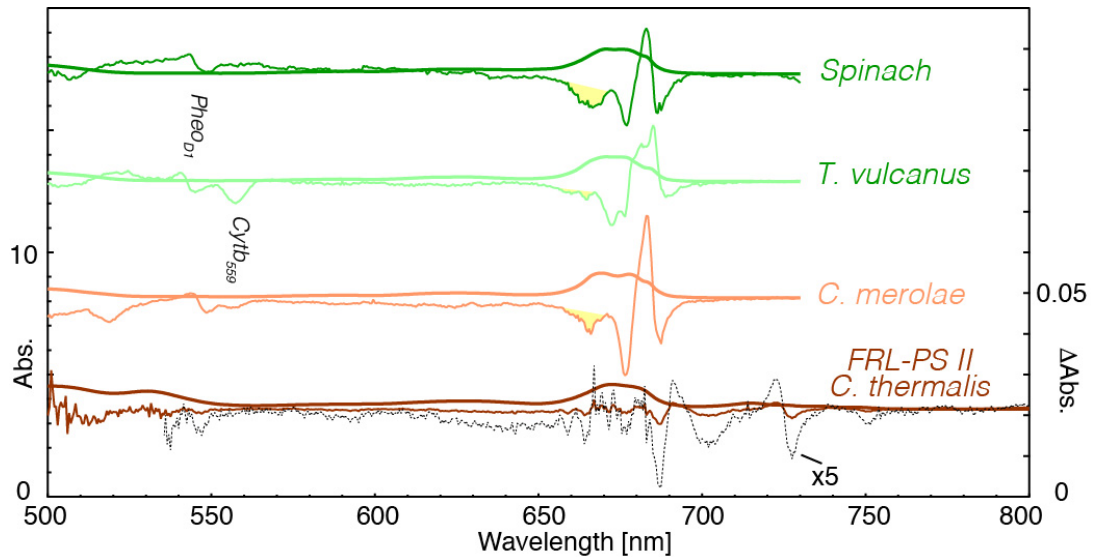
Fig. S5 *Absorption (left Scale) and illumination-induced difference spectra (right scale) for PS II core complexes derived from Spinach, T. vulcanus [13], C. merolae [14] and FRL C. thermalis [15] at 77 K. The shaded yellow regions are assigned to $ChlZ_{D2}$ bleaching (see text). Green light illumination fluences were standardized at 300 s of 5 mW/cm². Spectra have been scaled to comparable Q_y absorption intensities and offset for viewing. $Q_A^{\bullet-}$ yields in the first three systems are similar (60-80%), whereas the corresponding yield in FRL-PS II is ~10 to 20 times less.*

Low temperature electrochromic shifts associated with $Q_A^{\bullet-}$ formation have been extensively studied [16-21]. In Fig. S5, similar Q_x 'C550' electrochromic blue-shifts [16] of $Pheo_{D1}$ are evident in all organisms. The nearby bleach feature associated with oxidation of reduced $cytb_{559}$ is evident in *T. vulcanus* and *C. merolae* preparations. The FRL-PS II preparation of *C. thermalis* used for Fig. S5 did not contain a significant fraction of reduced $cytb_{559}$ and thus no bleach is seen, although this spectral feature was evident at 556.5 nm in other sample preparations (see Fig. S6 and [15]). Fig. S5 also shows the bleach near 666 nm, highlighted as a shaded yellow region, associated with the oxidation of a *chl-a* (often considered to be $ChlZ_{D2}$) for the first three organisms. This oxidation process appears less pronounced in FRL-PS II and other secondary donors such as β-carotenes may be involved [22-24].

The dominant electrochromic features in the Q_y region for *chl-a*-PS II have been identified as a red shift of $Pheo_{D1}$ near 680 nm and blue shift of Chl_{D1} Q_y near 685 nm. The precise position

and shape of shift features vary with organism. This variation is due to both small changes in pigment site energies with organism, along with changes in the effects of excitonic interactions between pigments associated with relatively small changes in their site energies. This is because the relative energy of sites can be changed quite significantly with respect to the exciton coupling matrix element between pigments. Shift features are doubled in some preparations of *T. vulcanus and T. elongatus i.e.* when there are two forms of the D1 protein expressed in the sample [25].

In the FRL-PS II Q_y region, the largest shifted feature is well separated with an intense blue shift feature occurring at 726 nm [15]. Compared to the data in Fig. S5, which are taken at 77 K, those taken at 1.8 K (Fig. 2 and Fig. 4 of manuscript) show better-resolved shift features.
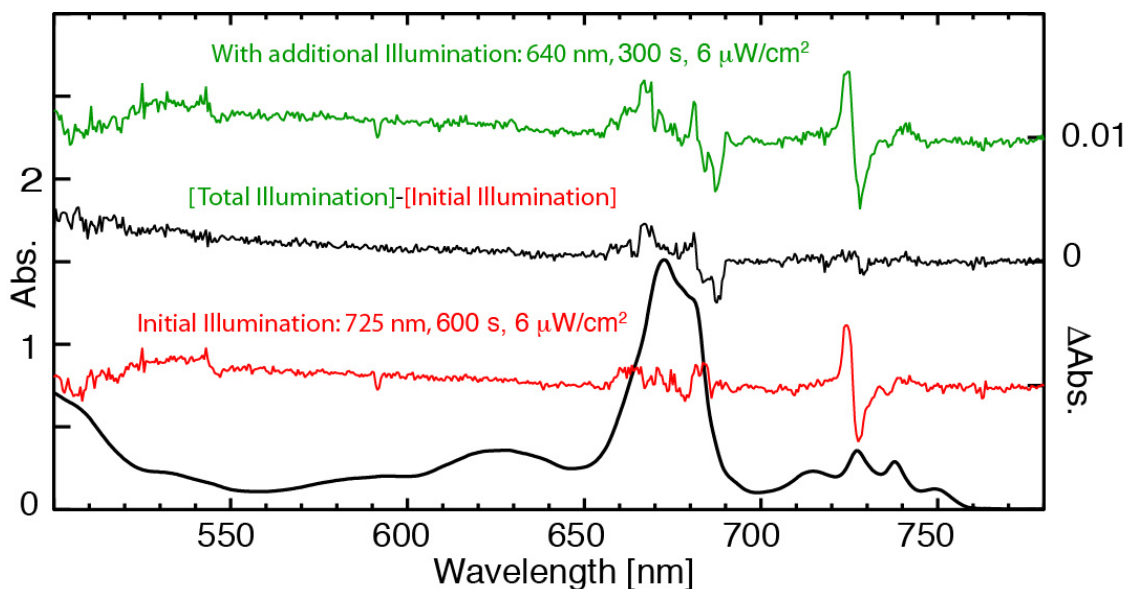

Fig. S6. *The bottom black trace is the absorption spectrum (left. scale) of the low-allophycocyanin FRL PS II core complex at 1.8 K. The red trace is the electrochromism spectrum (right scale) induced by illumination at 725 nm with the fluence indicated. The green trace is the accumulated electrochromism after an additional illumination at 640 nm. The thin black trace is the change in electrochromism induced by the 640 nm illumination component.*

FRL-PS II core samples contain some *chl-a*-PS II, as evidenced by its characteristic emission spectrum appearing in Fig. 1 of the main manuscript. FRL-PS II samples illuminated with light

at wavelengths significantly shorter than 700 nm, such as the green light used to generate difference spectra in Fig. S5, can be expected to display electrochromism associated with the *chl-a*-PS II component, as well as that of the (majority) FRL PS II component. Illumination of *chl-a*-PS II at 725 nm and 1.8 K is known to induce $Q_A^{\bullet-}$ formation (and as evidenced by electrochromism) but with low quantum efficiency [20, 26]. The *chl-a*-PSII electrochromism induced by illumination in the 700 nm to 730 nm range is due to absorption by the weak and broad, deep-red charge transfer state of *chl-a*-PS II [14, 20, 26].

Fig. S6 demonstrates that illumination of a low allophycocyanin FRL-PS II core complex sample with 640 nm light, following initial illumination at 725 nm, induces minimal additional electrochromism at 726 nm. The light-induced $Q_A^{\bullet-}$ formation of the FRL PS II component was essentially completed by the first illumination. However, additional 640 nm illumination leads to an electrochromism spectrum with a negative feature near 686 nm and a positive component near 682 nm. The spectrum exhibits low signal to noise as it was generated as a double-difference spectrum and also recorded in a region of high and rapidly varying absorbance. However, the pattern is compatible with it being due to the Chl_{D1} blue-shift of *chl-a*-PS II *of C. thermalis* [15]. For comparison, the $Q_A^{\bullet-}$ induced electrochromic shift of *T. vulcanus* (Fig. S5), a *chl-a* PS II thermophilic cyanobacterium has negative and positive peaks at 688 nm and 684 nm respectively.

The red trace in Fig. S6 shows no evidence of the negative feature seen near 685 nm in the black trace. We can conclude that no significant component of the *chl-a*-PS II contaminant of the FRL-PS II sample is photoconverted by 725 nm light. The electrochromism pattern in the red trace is then due only to the FRL PS II majority component in the sample.

The linewidth of the 726 nm feature (7 nm or ~130 cm^{-1} FWHM) allows an initial estimate of the electrochromic shift to be determined, independent of knowledge of the $Q_A^{\bullet-}$ yield. By measuring the offset, δ, of the derivative of the (initial) absorption spectrum compared to the

electrochromic shift feature, the electrochromic shift would then be 2δ, i.e. 2.2 nm or equivalently 42 cm^{-1}. This assumes that the relatively small fraction of FRL PS II that undergoes photoconversion has the same spectral distribution as the majority. Those FRL-PS II centers that are not photo-converted to the trapped $Q_A^{\bullet-}$ form do not contribute to the shift feature. The shift feature has a crossing point independent of yield as seen in Fig. S7, and is displaced 1.1 nm from the peak of the absorption, taken before illumination.

A $Q_A^{\bullet-}$ yield can then be estimated by simulating a 100% yield shift feature at 726 nm. This artificial, full-yield spectrum is generated by shifting the absorption spectrum taken before illumination to the blue by 2.2 nm. Subtracting the shifted spectrum from the initial spectrum yields a spectrum corresponding to the entire 726 nm feature being affected. Scaling this shift feature against the experimental 726 nm shift amplitude then provides a $Q_A^{\bullet-}$ yield. Fig. S7 shows fluence-dependent shift spectra with the apparent yield saturating at 10% when using 6 μW/cm^2 excitation at 725 nm.
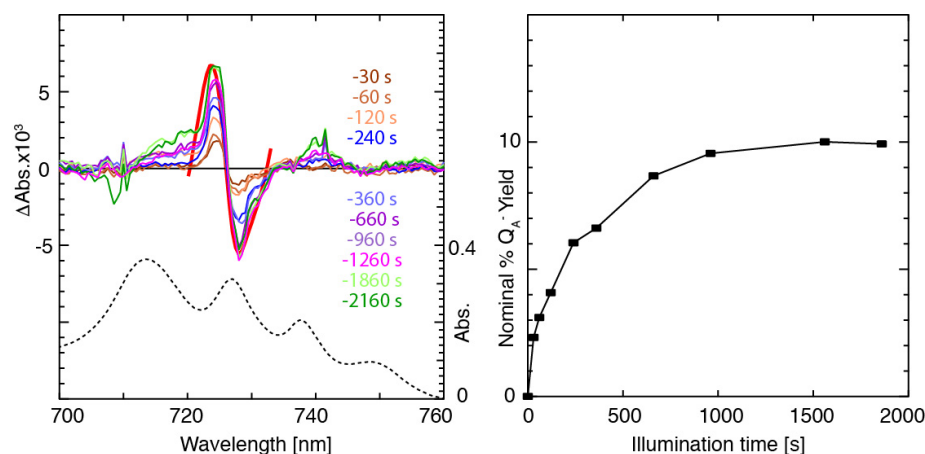

Fig. S7. *The left panel shows the fluence dependence of the electrochromic shift of high-allophycocyanin FRL-PS II at 1.8 K illuminated with 6 μW/cm^2 power density light at 725 nm. The red trace in the 726 nm region is the synthetic shift feature created by displacing the initial absorption spectrum by 2.2 nm (42 cm^{-1}) to the blue and subtracting this from the original spectrum. The right panel is the nominal yield of photoconversion to the $Q_A^{\bullet-}$ form of the enzyme versus illumination time, assuming a 2.2 nm electrochromic shift (see revision in text).*

At the lowest yields, a simple 726 nm shift feature dominates. It is narrower than the synthetic shift feature. At higher fluences, shoulders develop which may be associated with photoconversion of a population of FRL-PS II that exhibits the full primary donor spectral distribution. The initial slope of the conversion curve in Fig S7 can be analyzed by gauging the number of absorbed photons for a given excitation fluence. This leads to a direct estimate of the initial quantum efficiency of the $Q_A{}^{\bullet-}$ conversion as being close to unity. Such high initial quantum efficiencies were also seen in previous studies on spinach PS II core complexes [20] by monitoring the amplitude of the Q_x shift of $Pheo_{D1}$.

However, at 77 K, shift features at both high and low fluence are displaced from the peak maximum by 0.5 nm, whilst a corresponding synthetic shift feature generated by a 0.5 nm displacement of the 77 K 726 nm absorption accurately reproduces the shift feature shape. This revised estimate of the shift of 0.5 nm leads to a corresponding 2 x increase in our estimate of the $Q_A{}^-$ yield (i.e. to 20%), compared to that proposed in Fig. S7.

As mentioned above, the low fluence shift feature at 1.8 K arises from a narrower component of the overall primary donor inhomogeneous absorption profile. This narrower component is displaced by 1.1 nm from the peak maximum. This displacement, combined with an actual electrochromic shift of 1 nm, leads to the observed 1.8 K value of 2δ of 2.2 nm. The narrower component has a linewidth close to 4 nm, rather than the overall linewidth of 7-8 nm as given in Table S1. This narrower component of Chl-4 is more in line with the width observed for the Chl_{D1} site energy linewidth in the *chl-a*-PS II core complex (from spinach), which is 1.6 nm (Table S2).

SI-5 Exciton Modelling

Here, we used the same methodology previously used to model the PS II reaction center as present in core complexes of a number of organisms [27] and also for *isolated* PS II (RC-6 and RC-5) [10, 28] reaction centers. We calculated absorption and CD spectra of a range of

possible configurations of FRL-PS II. Apart from the single FRL chl site, the reaction center

parameters used were those for *chl-a*-PS II core complexes isolated from spinach as shown in

Table S2. The coupling matrix used is provided in Table S3.

Table S2

Spinach Core Complex PS II reaction center site parameters

	Site Energy nm/cm^{-1}	FWHM Linewidth nm/cm^{-1}
Chl$_{D1}$	684/14620	1.6/40
Pheo$_{D2}$	678/14750	4.0/100
Pheo$_{D1}$	676.5/14780	5.6/140
P$_{D1}$	668.5/14960	6.3/140
P$_{D2}$	668.5/14960	6.3/140
Chl$_{D2}$	669/14950	6.1/140
ChlZ$_{D1}$	672/14880	6.1/140
ChlZ$_{D2}$	665/15040	6.1/140

Table S3

PS II reaction center exciton coupling matrix elements [29]

Coupling (cm^{-1})	Chl$_{D1}$	Pheo$_{D2}$	Pheo$_{D1}$	P$_{D1}$	P$_{D2}$	Chl$_{D2}$	ChlZ$_{D1}$	ChlZ$_{D2}$
Chl$_{D1}$	0	-2.18	43.51	-27.32	-46.77	3.54	1.67	-0.09
Pheo$_{D2}$	-2.18	0	1.55	12.61	-2.99	41.65	-0.19	-2.57
Pheo$_{D1}$	43.51	1.55	0	-3.96	15.06	-2.37	-2.52	-0.18
P$_{D1}$	-27.32	12.61	-3.96	0	158	-41.83	0.45	0.58
P$_{D2}$	-46.77	-2.99	15.06	158	0	-22.04	0.6	0.61
Chl$_{D2}$	3.54	41.65	-2.37	-41.83	-22.04	0	-0.05	1.8
ChlZ$_{D1}$	1.67	-0.19	-2.52	0.45	0.6	-0.05	0	0.15
ChlZ$_{D2}$	-0.09	-2.57	-0.18	0.58	0.61	1.8	0.15	0

Transition dipole strengths were taken from reference [30] as 5.47 D for *chl-a* and 4.25 D for

pheo-a and structural data determined from crystal structure data [31].

Electrochromic shifts, Δ, induced by reducing Q_A and $Pheo_{D1}$ forming their anion radical states, can be modelled by considering the interaction of $\overrightarrow{\Delta\mu}$ of each reaction center pigment with the electric field associated with a point charge at the position of the reduced species.

$$\Delta = \frac{\overrightarrow{\Delta\mu} \cdot e}{|\vec{r}|^2}$$

A starting point [30, 32, 33] is to assign $\Delta\mu$ to be 1.8 D for all *chl-a* Q_y excitations and 1.35 D for *pheo-a* Q_y excitations, with *e* being the electronic charge. This shift, Δ, is then reduced to Δ/f because of the influence of the local dielectric in the protein. When *f* is taken as 3, the site energy shifts are as given below.

Table S4

PS II Reaction Center Site Energy Shifts for f = 3

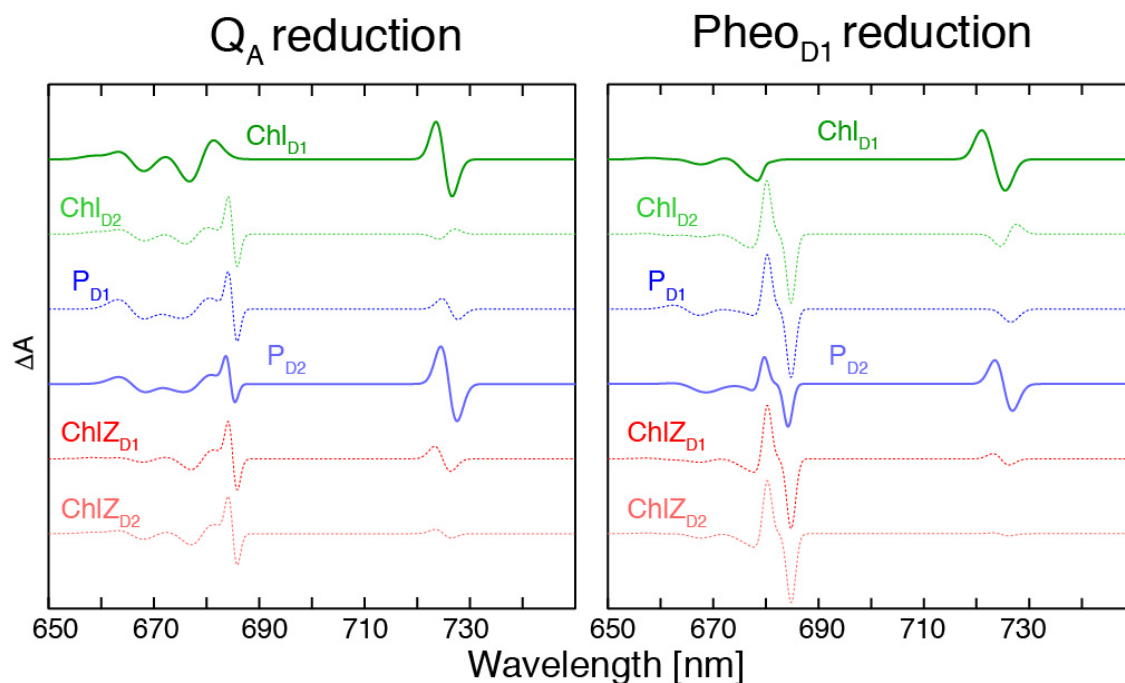| Shift/cm^{-1}	$Q_A^{\cdot-}$	$Pheo_{D1}^{\cdot-}$
Chl$_{D1}$	14.4	77.2
Pheo$_{D2}$	-9.6	-0.1
Pheo$_{D1}$	-53.8	
P$_{D1}$	5.8	0.4
P$_{D2}$	18.0	45.1
Chl$_{D2}$	-5.4	-18.8
ChlZ$_{D1}$	10.0	11.2
ChlZ$_{D2}$	3.9	2.8

Fig. S8 *Left and right panels show calculated electrochromic shift patterns induced by an electron located at the Q_A and $Pheo_{D1}$ positions, respectively. Shift patterns were calculated using the parameters in Tables S2 and S3. Calculations are presented for all locations of a single FRL chlorophyll in the reaction center. The two cases which induce an electrochromic shift near 726 nm compatible with experimental data (Chl_{D1} and P_{D2}) are accentuated (thicker solid lines).*

The calculated electrochromic patterns shown in Fig. S8 indicate that $Pheo_{D1}$ reduction experiments could assist in discriminating between the Chl_{D1} and P_{D2} locations for the primary donor. A relatively large primary donor shift for the Chl_{D1} assignment is calculated for the $Pheo_{D1}$ reduction compared to that for the $Q_A^{\cdot-}$ reduction. More useful may be that the associated electrochromic pattern seen in the *chl-a* Q_y spectral region is different for the Chl_{D1} and P_{D2} primary donor assignments. The room temperature $Pheo_{D1}$ reduction spectra previously published in Fig 2D of [15] display a broad negative feature at 658 nm as well a stronger broad positive feature near 650 nm. Neither of these features correspond to the calculated electrochromism (see Fig. S8). In experiments [27, 35] on canonical *chl-a*-PS II preparations, there is no evidence of broad features similar to those seen in Fig. 2D of ref

[15]. It thus seems important to generate the trapped Pheo$^-$ state at low temperature in future experiments.
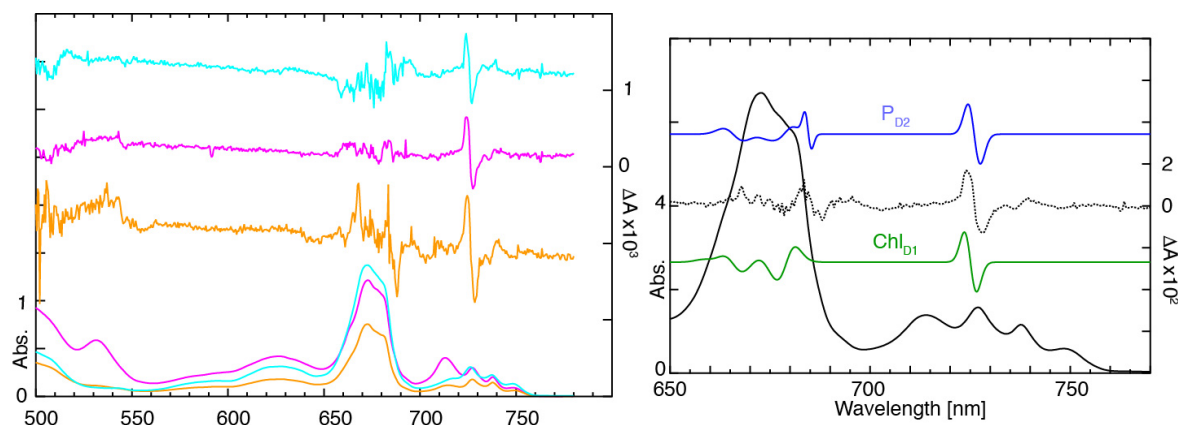

Fig. S9 *The left panel shows the absorption (lower traces) and electrochromic shift patterns (each offset for clarity) induced by 725 nm illumination at 1.8 K of three different FRL PS II core complex samples having various allophycocyanin content. The right panel shows the sum of the three absorption spectra (thick black trace) and the sum of the corresponding three electrochromism spectra (thin black trace). Also shown are the calculated electrochromic patterns (from Fig. S8) when the primary donor is located at ChlD1 (green trace) and PD2 (blue trace). For both cases the calculated patterns have been scaled to match the experimental electrochromism amplitude.*

The signal-to-noise ratio and other limitations in the in the 725 nm-induced electrochromism spectra presented in Figs, 2 and 4 of the manuscript and in Fig. S9 makes it difficult to determine which calculated Q_A reduction pattern calculated (Fig. S8) better fits the experimental data in the *chl-a* region. Fig. S9 addresses this difficulty by adding results from identical experiments performed on three different FRL-PS II samples exhibiting differing allophycocyanin concentrations. Illuminations were performed with an identical fluence of 6 µW/cm² at a wavelength of 725 nm for 300s. This illumination protocol is shown to correspond to conditions where no significant *chl-a* based photochemistry is induced (see Fig. S6), i.e. that associated with *chl-a*-PS II present in the samples. A comparison of the averaged shift pattern with those calculated for the 680 nm region appears to be more compatible with P_{D2}

being the primary donor. The main feature at ~ 680 nm appears experimentally as a blue shift,

as calculated for the P_{D2} case, rather than a red shift as calculated for the Chl_{D1} case.

References

[1] R. MacColl, L.E. Eisele, A. Menikh, Allophycocyanin: Trimers, monomers, subunits, and homodimers, Biopolymers, 72 (2003) 352-365.

[2] E. Krausz, J.L. Hughes, P. Smith, R. Pace, S. Peterson Årsköld, Oxygen-Evolving Photosysten II Core Complexes: A New Paradigm Based on the Spectral Identification of the Charge-Separating State, the Primary Acceptor and Assignment of Low-Temperature Fluorescence, Photochemical and Photobiological Sciences, 4 (2005) 744-753.

[3] M.-L. Groot, R.N. Frese, F.L. de Weerd, K. Bromek, A. Pettersson, Spectroscopic Properties of the CP43 Core Antenna Protein of Photosystem II, Biophysical Journal, 77 (1999) 3328-3340.

[4] M.L. Groot, E.J.G. Peterman, I.H.M. Vanstokkum, J.P. Dekker, R. Vangrondelle, Triplet and Fluorescing States of the Cp47 Antenna Complex of Photosystem-Ii Studied as a Function of Temperature, Biophysical Journal, 68 (1995) 281-290.

[5] E. Krausz, J.L. Hughes, P.J. Smith, R.J. Pace, S. Peterson Årsköld, Assignment of the low-temperature fluorescence in oxygen-evolving Photosystem II, Photosynthesis Research, 84 (2005) 193-199.

[6] T. Renger, E. Schlodder, Optical properties, excitation energy and primary charge transfer in photosystem II: Theory meets experiment, J Photoch Photobio B, 104 (2011) 126-141.

[7] M. Mimuro, M. Kobayashi, K. Shimada, K. Uezono, T. Nozawa, Magnetic Circular Dichroism Properties of Reaction Centre Complexes Isolated from the Zinc-Bacteriochlorophyll *a*-containing Bacterium *Acidiphilium rubrum*, Biochemistry, 39 (2000) 4020-4027.

[8] P.J. Smith, S. Peterson, V.M. Masters, T. Wydrzynski, S. Styring, E. Krausz, R.J. Pace, Magneto-Optical Measurements of the Pigments in Fully Active Photosystem II Core Complexes from Plants, Biochemistry, 41 (2002) 1981-1989.

[9] E. Krausz, Selective and differential optical spectroscopies in photosynthesis, Photosynthesis Research, 116 (2013) 411-426.

[10] J. Hall, R. Picorel, N. Cox, R. Purchase, E. Krausz, New Perspectives on Photosystem II Reaction Centres, Australian Journal of Chemistry, in press DOI: 10.1071/CH19478 (2020).

[11] H. van Amerongen, R. van Grondelle, L. Valkunas, Photosynthetic Excitons, WORLD SCIENTIFIC, 2000.

[12] O.D. Canaani, E. Gantt, Circular-Dichroism and Polarized Fluorescence Characteristics of Blue-Green-Algal Allophycocyanins, Biochemistry, 19 (1980) 2950-2956.

[13] S. Peterson Årsköld, P.J. Smith, J.-R. Shen, R.J. Pace, E. Krausz, Key Cofactors of Photosystem II Cores from Four Organisms Identified by 1.7-K Absorption, CD, and MCD, Photosynthesis Research, 84 (2005) 309-316.

[14] J. Langley, J. Morton, R. Purchase, L. Tian, L. Shen, G. Han, J.R. Shen, E. Krausz, The deep red state of photosystem II in Cyanidioschyzon merolae, Photosynthetica, 56 (2018) 275-278.

[15] D.J. Nurnberg, J. Morton, S. Santabarbara, A. Telfer, P. Joliot, L.A. Antonaru, A.V. Ruban, T. Cardona, E. Krausz, A. Boussac, A. Fantuzzi, A.W. Rutherford, Photochemistry beyond the red limit in chlorophyll f-containing photosystems, Science, 360 (2018) 1210-1213.

[16] W.L. Butler, Primary Photochemistry of Photosystem II of Photosynthesis, Accounts of Chemical Research, 6 (1973) 177-184.

[17] D.H. Stewart, P.J. Nixon, B.A. Diner, G.W. Brudvig, Assignment of the Q_y Absorbance Bands of Photosystem II Chromophores by Low-Temperature Optical Spectroscopy of Wild-Type and Mutant Reaction Centres, Biochemistry, 39 (2000) 14583-14594.

[18] S. Peterson Årsköld, V.M. Masters, B.J. Prince, P.J. Smith, R.J. Pace, E. Krausz, Optical Spectra of Synechocystis and Spinach Photosystem II Preparations at 1.7 K: Identification of the D1-Pheophytin Energies and Stark Shifts, Journal of the American Chemical Society, 125 (2003) 13063-13074.

[19] J.L. Hughes, B.J. Prince, E. Krausz, P.J. Smith, R.J. Pace, H. Riesen, Highly Efficient Spectral Hole-Burning in Oxygen-Evolving Photosystem II Preparations, Journal of Physical Chemistry B, 108 (2004) 10428-10439.

[20] J.L. Hughes, P. Smith, R. Pace, E. Krausz, Charge Separation in Photosystem II Core Complexes Induced by 690-730 nm Excitation at 1.7 K, Biochimica et Biophysica Acta, 1757 (2006) 841-851.

[21] E. Schlodder, T. Renger, G. Raszewski, W.J. Coleman, P.J. Nixon, R.O. Cohen, B.A. Diner, Site-directed Mutations at D1-Thr179 of Photosystem II in Synechocystis sp. PCC 6803 Modify the Spectroscopic Properties of the Accessory Chlorophyll in the D1-branch of the Reaction Center, Biochemistry, (2008).

[22] P. Faller, A. Pascal, A.W. Rutherford, Beta-carotene redox reactions in photosystem II: electron transfer pathway, Biochemistry, 40 (2001) 6431-6440.

[23] T. Cardona, A. Sedoud, N. Cox, A.W. Rutherford, Charge separation in Photosystem II: A comparative and evolutionary overview, Biochimica et Biophysica Acta, (2011).

[24] T. Wydrzynski, K. Satoh, Photosystem II - The Light-Driven Water:Plastoquinone Oxidoreductase in: Govindjee (series ed), Advances in Photosynthesis and Respiration Vol. 22 pp 786. Springer, Dordrecht, The Netherlands., 2005.

[25] M. Sugiura, C. Azami, K. Koyama, A.W. Rutherford, F. Rappaport, A. Boussac, Modification of the pheophytin redox potential in Therrnosynechococcus elongatus Photosystem II with PsbA3 as D1, Bba-Bioenergetics, 1837 (2014) 139-148.

[26] J. Morton, J. Hall, P. Smith, F. Akita, F.H. Koua, J.R. Shen, E. Krausz, Determination of the PS I content of PS II core preparations using selective emission: a new emission of PS II at 780nm, Biochim Biophys Acta, 1837 (2014) 167-177.

[27] N. Cox, J.L. Hughes, R. Steffen, P.J. Smith, A.W. Rutherford, R.J. Pace, E. Krausz, Identification of the Q(Y) Excitation of the Primary Electron Acceptor of Photosystem II: CD Determination of Its Coupling Environment, Journal of Physical Chemistry B, 113 (2009) 12364-12374.

[28] N. Cox, J. Hughes, A.W. Rutherford, E. Krausz, On the assignment of PSHB in D1/D2/cytb(559) reaction centers, Physcs Proc, 3 (2010) 1601-1605

1100.

[29] F. Muh, M. Plockinger, T. Renger, Electrostatic Asymmetry in the Reaction Center of Photosystem II, J Phys Chem Lett, 8 (2017) 850-858.

[30] V.I. Novoderezhkin, J.P. Dekker, R. van Grondelle, Mixing of Exciton and Charge-Transfer States in Photosystem II Reaction Centers: Modeling of Stark Spectra with Modified Redfield Theory, Biophys. J., 93 (2007) 1293-1311.

[31] Y. Umena, K. Kawakami, J.R. Shen, N. Kamiya, Crystal structure of oxygen-evolving photosystem II at a resolution of 1.9 angstrom, Nature, 473 (2011) 55-U65.

[32] G. Raszewski, W. Saenger, T. Renger, Theory of Optical Spectra of Photosystem II Reaction Centers: Location of the Triplet State and the Identity of the Primary Electron Donor, Biophysical Journal, 88 (2005) 986-998.

[33] G. Raszewski, B.A. Diner, E. Schlodder, T. Renger, Spectroscopic properties of reaction center pigments in photosystem II core complexes: Revision of the multimer model, Biophysical Journal, 95 (2008) 105-119.

[34] R.N. Frese, M. Germano, F.L. de Weerd, I.H.M. van Stokkum, A.Y. Shkuropatov, V.A. Shuvalov, H.J. van Gorkom, R. van Grondelle, J.P. Dekker, Electric Field Effects on the Chlorophylls, Pheophytins, and β-Carotenes in the Reaction Center of Photosystem II, Biochemistry, 42 (2003) 9205-9213.

[35] V.V. Klimov, A.V. Klevanik, V.A. Shuvalov, A.A. Krasnovsky, Reduciton of Pheophytin in the primary light reaction of Photosystem II., FEBS Lett., 82 (1977) 183-186.